

# **The Atacama Compact Array System**

## **Project Description**

***Draft Version 1***

**February 17, 2004**

National Astronomical Observatory  
of Japan

# TABLE OF CONTENTS

1. Introduction
2. Science Cases
  - 2.1 Key role of ACA in Mosaicing with ALMA
  - 2.2 Enhanced Science with ACA
3. Science Requirements
  - 3.1 General Requirements
  - 3.2 Specific Requirements
  - 3.3 The ACA System in the Early Science Observations
4. Operations of the ACA system
  - 4.1 Joint Operation of ALMA Including the ACA System
  - 4.2 Coordinated Science Operations of the 64-element Array and the ACA System
  - 4.3 Operation and Maintenance of the ACA System at AOS and OSF
5. ACA System Design
  - 5.1 Introduction
  - 5.2 Calibration Method
  - 5.3 Configuration
  - 5.4 Antennas
  - 5.5 Front End Subsystem
  - 5.6 Local Oscillators
  - 5.7 Backend Subsystem
  - 5.8 Correlator
  - 5.9 Computing
  - 5.10 Site Development

# Introduction

Tetsuo Hasegawa

## Revision History

2003-06-02: First draft

The Atacama Compact Array (ACA) system is built as a contribution of Japan to the ALMA project, and is designed for use as a part of the entire ALMA system in the early and full science operations phases. It is composed of an array of twelve 7-m dishes and four 12-m dishes. The 7-m antennas are packed in a very compact configuration to take short baseline data corresponding to the low spatial frequency Fourier components of the brightness distribution of the observed sources. The 12-m antennas are capable of taking single-dish images that contain information of the Fourier components of even lower spatial frequencies (down to zero ideally). These data are combined with the data from the 64-element array of 12-m antennas in the data processing software to make the final mosaic image of the sources.

Mosaicing is a technique that allows mapping of an area of the sky that is larger than the beam of the array elements (e.g., Thompson, Moran, and Swenson 2001). It is very important for millimeter and submillimeter wavelength interferometers, because the beams of the element antennas are relatively narrow. Many astronomical studies require a comparison of images with a wide range of spatial scales, and it is expected that a significant fraction of observing programs at large millimeter/submillimeter arrays will require mosaicing observations.

ALMA is one of the first millimeter/submillimeter arrays that incorporate the requirements for mosaicing in their concepts, and a number of design studies have been made in order to realize the mosaicing capability in the millimeter and submillimeter imaging. For imaging objects larger than the primary beam of the element antennas, a combination of single-dish and interferometer data is required (Cornwell 1988). Cornwell, Holdaway, and Uson (1993) showed that mosaiced images with a homogeneous array combined with the single-dish data taken with the element antenna(s) can sample, in principle, all spatial frequencies between zero and the maximum interferometer baseline. This is possible because the multiple pointing of the interferometer antennas extends the  $uv$  coverage of close pairs inside the circle of one antenna diameter, which overlaps with the  $uv$  coverage provided by the single-dish map (Ekers and Rots 1979; Welch 1995). However, pointing errors of the element antennas spoil this procedure. Cornwell, Holdaway, and Uson (1992) has pointed out

that only small pointing and surface errors ( $\sim 6\%$  of HPBW and  $\sim 1/40$ ) are allowed for a homogeneous array to reproduce images of very large sources with high dynamic range ( $>1000$ ) and fidelity ( $\sim 20$ ). Holdaway (1997) simulated the mosaicing performance of ALMA taking the pointing errors due to wind and other causes into account, and showed that the fidelity of the reconstructed images is limited by the pointing errors. Systematic errors shared by the antennas were found to be particularly harmful.

ACA was conceived to solve this problem. The addition of a compact array of smaller high precision antennas allows direct sampling of shorter  $uv$  spacings. This will reliably recover more of the total flux density and the large-scale structure even at submillimeter wavelengths (Wright 1999). An approach to decide the number of the smaller antennas is to require that the point source sensitivity of the compact array be comparable with that of an equal area annulus at the inner edge of the 12-m  $uv$  coverage (Welch 2000). The required number of small antennas is approximately  $(12/D_c)/6$ , where  $D_c$  [m] is the diameter of the small antennas. A traditional choice for the diameter  $D_c$  may be 6 m, a half of 12 m, although there are other issues to be considered. If we choose a smaller  $D_c$ , we need to spend increasingly more time in calibration during observations. Smaller  $D_c$  also increases the number of the small antennas increasing cost of receivers, the correlator, antenna pads, etc. With these issues considered, it has become a consensus that the compact array will be composed of twelve 7-m antennas. The sensitivity argument requires four dedicated 12-m antennas for single-dish mapping (e.g., Welch 2003). When we calibrate the antennas in the compact array, these four 12-m antennas join to enhance the sensitivity. The ACA System includes both the compact array of twelve 7-m antennas (ACA) and the four 12-m antennas for single-dish mapping.

Intensive simulation studies have been made to assess the impact of the ACA to the wide-field imaging capability of ALMA (Yun 2001; Morita 2001; Pety, Gueth, and Guilloteau 2001a; Pety, Gueth, and Guilloteau 2001b; Pety, Gueth, and Guilloteau 2001c). These studies have led to a common conclusion that the addition of ACA provides robust results, when ALMA without ACA would fail in presence of pointing and phase errors, or on some types of images.

In line with the simulations described above, the ALMA Science Advisory Committee (ASAC) has made a focused effort to evaluate the benefit of ACA to the science with ALMA. The result was summarized in the ASAC report (October 2001) and the document “Scientific Justification for the ALMA Enhancements” attached to the report. In addition to the enhancement of the imaging performance of ALMA, the scientific benefit of ACA serving, for a fraction of time, as a stand-alone submillimeter-wave array was noted. The report ranked the ACA as *Top Priority* along with Band 10 among possible enhancements for the 3-way ALMA project.

The present document, **Part 1** (Chapter 1 to 5) of the Project Description of the ACA System, describes the science cases of the system, its science requirements, top level technical specifications derived from the science requirements, and the system design. **Part 2** of the Project Description of the ACA System will follow, and it will describe the implementation plan for the ACA System including the detailed design of its individual subsystems, the schedule for construction and commissioning, and a detailed plan for its operation.

## References

- Cornwell, T. J., 1988, "Radio-interferometric imaging of very large objects", A&A 202, 316.
- Cornwell, T. J., Holdaway, M. A., and Uson, J. M., 1993, "Radio-interferometric imaging of very large objects: implications for array design", A&A 271, 697.
- Ekerts, R. D., and Rots, A. H., 1979, in Proc. IAU Colloq. 49, C. van Schooneveld, ed., (D. Reidel) p. 61.
- Holdaway, M. A., 1997, MMA Memo 178, "Effects of Pointing Errors on Mosaic Images with 8 m, 12 m, and 15 m Dishes".
- Morita, K.-I., 2001, ALMA Memo 374, "Wide Field Imagings with the Atacama Large Millimeter/Submillimeter Array".
- Pety, J., Gueth, F., and Guilloteau, S., 2001a, ALMA Memo 386, "ALMA+ACA Simulation Tool".
- Pety, J., Gueth, F., and Guilloteau, S., 2001b, ALMA Memo 387, "ALMA+ACA Simulation Results".
- Pety, J., Gueth, F., and Guilloteau, S., 2001c, ALMA Memo 398, "Impact of ACA on the Wide-Field Imaging Capabilities of ALMA".
- Thompson, A. R., Moran, J. M., and Swenson, Jr., G. W., 2001, "Interferometry and Synthesis in Radio Astronomy", 2<sup>nd</sup> ed. (John Wiley & Sons, Inc.).
- Welch, W. J., 1995, MMA Memo 134, "Some Comments on Sampling, Antenna Spacings, and uniform Aperture Illumination".
- Welch, W. J., 2000, ALMA Memo 354, "Choices of Antenna Size and Number for the Atacama Compact Array".
- Welch, W. J., 2003, ALMA Memo 454, "Total Power Observing with the ALMA Antennas".
- Wright, M. C. H., 1999, ALMA Memo 272, "Image Fidelity: Implications for ALMA".
- Yun, M., 2001, ALMA Memo 368, "An imaging Study for ACA"

# Science Case

Ken Tatematsu and Tetsuo Hasegawa

## Revision History

2003-08-10: First Draft

2004-02-10: Added about DRSP statistics in 2.1.

## 2.1. Key Role of ACA in Mosaicing with ALMA

In aperture synthesis arrays, the field of view of the image taken with a single pointing is limited by the primary beam of the element antennas. **Table 2.1** shows the size of the primary beam of the 12 m element antenna at various observing frequencies that are important in ALMA science. As the observing frequency goes up, the field of view of the ALMA 12-m antenna array shrinks to a few tens of arcseconds or less. This field of view is not large enough for many of the important targets for ALMA, and multiple-pointing (mosaicing) observations are required to cover the full extent of sources. In addition, it has become a norm in contemporary astrophysics to compare images taken in various wavelengths across the electromagnetic spectrum. It has become common in some areas of astronomical observations that images taken contain a rich spectrum of spatial structures with spatial Fourier spectrum spanning a few to several orders of magnitudes. As a major instrument in the 21-st century, ALMA is expected to provide comparable wide-field high-resolution images with high level of fidelity and robustness. As reviewed in the previous section, the Atacama Compact Array (ACA) System has been conceived to enable ALMA to meet this expectation.

**Table 2.1:** Half-power beam width (HPBW) of the 12-m antennas that defines the field of view of ALMA in single pointing

Frequency (GHz)	HPBW (arcsec)
115	54
230	27
345	18
492	13
650	9
950	6

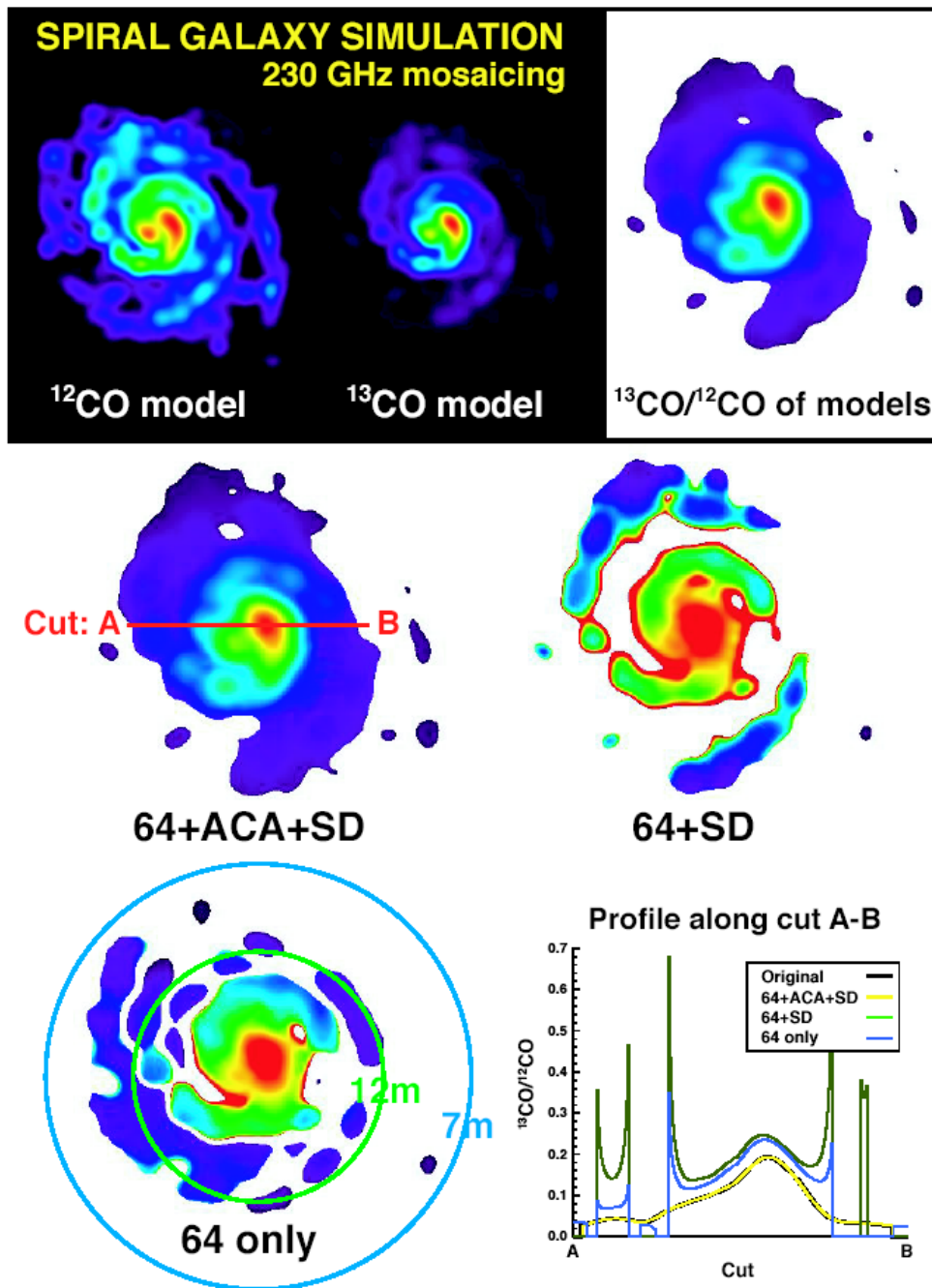
Table 2.2 lists examples of ALMA scientific programs which may be benefited by addition of ACA observations. This is an update of the table 2 in the ASAC report “Scientific Justification for the ALMA Enhancements” (October 15, 2001). At least about 50 % of the listed scientific targets can be benefited by ACA. Actual need of ACA would be judged with the required sensitivity and integration time taken in to account --- for example, galactic star forming regions with large angular extents are generally bright and the integration time required for a program tend to be relatively short, while resolving a forming galaxy at a large redshift would require a single-field observation with a long integration time. It is not easy to derive the precise percentage, but our experience suggests that no less than 25 % (measured in the 64-element array time) of the ALMA programs will require ACA data (the ASAC report 2001). This expectation is consistent with the statistics of the ALMA Design Reference Science Plan (DRSP) recently reported by ASAC, which shows that observing time requested to both the ACA and the 64-element array is about 41 % of total requested time for all the projects in DRSPs.

The importance of ACA in wide-field imaging with ALMA has been demonstrated by a series of imaging simulations as described in Chapter 1. Figure 2.1 shows a new simulation result. The simulation was carried out for  $^{12}\text{CO}$  (2-1) and  $^{13}\text{CO}$  (2-1) for the model spiral galaxy. One scientific interest in such observation is the arm/interarm column density contrast and its relation to the star formation activity. We derive the line intensity ratio, which reflects the column density. From the simulation result, it is obvious that ACA will lead to appreciable improvement in imaging quality. Without ACA, it would be impossible to derive physical properties such as temperature, density reliably from the line ratio measurements.

**Table 2.2:** Examples of ALMA programs with potential ACA contribution

Distance	Object	Linear Size	Apparent Size (")	Sample ALMA programs	ACA? submm mm
z~3-10	Proto galaxies	10 kpc	1-10	Blind survey of dust, CO, ...	Y N
z~1	Proto disk-galaxies	10 kpc	2	Blind survey of dust, CO, ...	N N
z~0.5-3	SZ effect	1 Mpc	200	Imaging SZ effect to determine H <sub>0</sub>	Y Y
z~0.5	Blue galaxies	10 kpc	2	Blind survey of dust, CO, CI, ...	N N
z~0.1-3	Ultraluminous IR gal	10 kpc	6	Imaing the structures, line ratios	Y N
z~0.01	Galaxies at z = 0.01	10 kpc	50	Imaging the structure, line ratios.	Y Y
10 Mpc	AGN tori	1 pc	0.01	Imaging of obscuring torus.	N N
10 Mpc	AGN circumnuclear region	50 pc	1	Structure and kinematics	N N
10 Mpc	AGN, starburst centers	1 kpc	20	Structure and kinematics	Y Y
10 Mpc	Nearby spiral galaxies	10 kpc	200	Imaging the structure, line ratio.	Y Y
1 Mpc	Nearby super massive BH	0.3 pc	0.06	Gas kinematics	N N
1 Mpc	Molecular clumps in nrby gal	1 pc	0.1	Star formation in galaxies	N N
50 kpc	GMC in LMC/SMC	100 pc	25	Line ratios, structure, mass spectr.	Y Y
50 kpc	Dense cores in LMC/SMC	0.3 pc	0.1	Star formation in low metallicity	N N
8 kpc	Galactic Center	5 pc	100	Mini spiral, continuum, lines	Y Y
5 kpc	Hot cores	0.05 pc	2	Line surveys, continuum	N N
5 kpc	UC HII	0.05 pc	2	Line surveys, continuum	N N
1 kpc	SNRs	0.05 pc	10	Line ratios, shock front structure	Y N
1 kpc	Late-type stars	0.02 pc	4	Line survey, radial profile	Y N
1 kpc	Cluster in cloud core	0.1 pc	20	Radial profile, polarimetry	Y Y
0.1-1 kpc	Molecular outflows	0.01-0.5pc	400	Kinematics, cavities, line ratios	Y Y
0.1 kpc	Infalling protostellar envelope	5000 AU	50	Radial profile, line ratios	Y Y
0.1 kpc	Proto-planetary disks	400 AU	4	Dust + molecules, gaps, line ratios	Y N
10-100 pc	Debris disk of MS stars	400 AU	4-40	Structure, gaps	Y Y
	Large planets		30	Structure of atmosphere	Y Y
	Smaller planets		<3	Structure of atmosphere	N N
	Comets		2-100	Jets, distributed molecules in coma	Y Y
	Sun		1800	Limb brightening, solar activity	Y Y





T. Tsutsumi, K. Tatematsu, K.-I. Morita, R. Kandori

**Figure 2.1:** Imaging simulation of  $^{12}\text{CO}$  (2-1) and  $^{13}\text{CO}$  (2-1) of the spiral galaxy with 7-field mosaic. The GILDAS software package was used. The image size is 54.8" square. The original image is constructed by image processing of the  $^{12}\text{CO}$  (1-0) image of M51 (Nakai et al. 1994).

## 2.2. Enhanced Science with ACA

In the following, we discuss the scientific examples which requires ACA, a) at submillimeter wavelengths, and b) at lower millimeter frequencies.

### a) Importance of ACA at submillimeter wavelengths

The ACA will be important at high frequency, because the field of view becomes smaller. At high frequencies like Bands 8-10, structures having sizes of order 5-10 arcsec or larger will be benefited by ACA. In particular, the dust continuum emission, the neutral atomic carbon emission, and the redshifted ionized carbon emission are spatially extended, and it is impossible to obtain the reliable images without ACA. Here, we list some examples which will be benefited by the ACA system.

#### a-1) Protogalaxies at submillimeter wavelengths

The galaxy is one of the basic elements of the universe. For understanding the history and evolution of the universe, it is essential to know how the galaxy forms. Observations at optical and near-infrared wavelengths have revealed the history of galaxies to some extents, but the formation process is hard to investigate only at these wavelengths because we cannot observe the material for the galaxies.

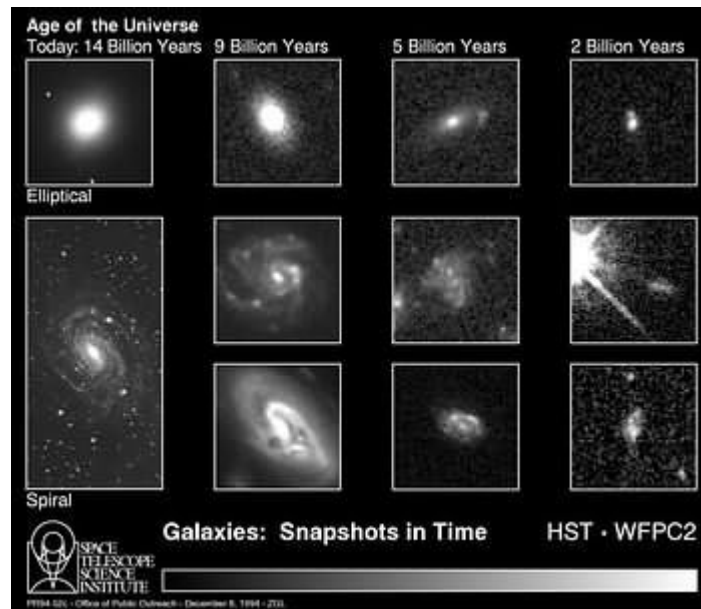


**Fig. 2.2:** Galaxies at various distances and ages (Dressler et al. 1994).

ALMA will make clear how galaxies form in the early universe with information of gas and dust. The key probes are the dust continuum emission and redshifted CII emission. Since 10 kpc

corresponds to 1-10 arcsec at  $z = 3-10$  depending on the deceleration parameter  $q_0$ , the field of view becomes of order the size of galaxy material at submillimeter wavelengths. It is quite essential to obtain the spatial information of the material of protogalaxies.

### a-2) Protoplanetary disks at Bands 8-10.

The planet formation is one of the major targets of ALMA. Dichroic or multi-color studies are essential for studies of its evolution. It is known that protoplanetary disks have smaller dust emissivity ( $\sim 1$ ) than the interstellar medium ( $\sim 2$ ). This is often explained in terms that dust grains coagulated in the protoplanetary disk. Because coagulation is the very essential process for the planet formation, it is of our great interest whether there is spatial variation of dust emissivity within the protoplanetary disk. To measure SED (spectral energy distribution) precisely, it is important to have lowest and highest frequency data. Continuum imaging quality at Band 10 is very crucial in this point. The protoplanetary disk with a size of 400 AU is 4 arcsec at a distance of 100 pc. It is also of great interest how the edge of the disk is connected to the interstellar matter (or parent cloud core). Without an aid of the ACA system, we will not be able to estimate variation of dust emissivity within the protoplanetary disk or to know how the outer disk is connected to the interstellar space reliably.

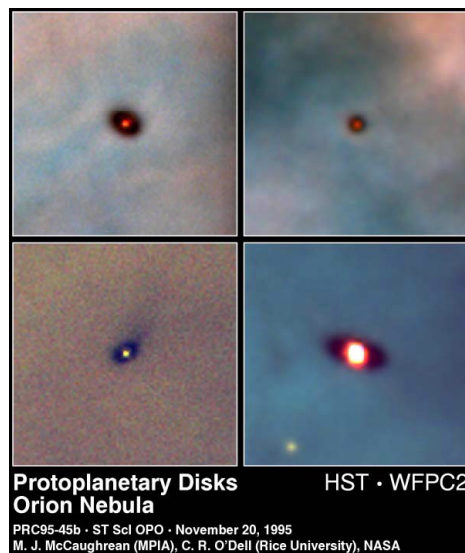


**Fig. 2.3:** HST images of protoplanetary disks (McCaughrean and O'Dell 1995). With ALMA, we can study the physical and chemical properties of the protoplanetary disk.

### a-3) CI in galaxies

Israel and Baas (2002) have demonstrated that CI/13CO(2-1) ratio increases with increasing galactic center activity (quiescent to strong starburst, and AGN).

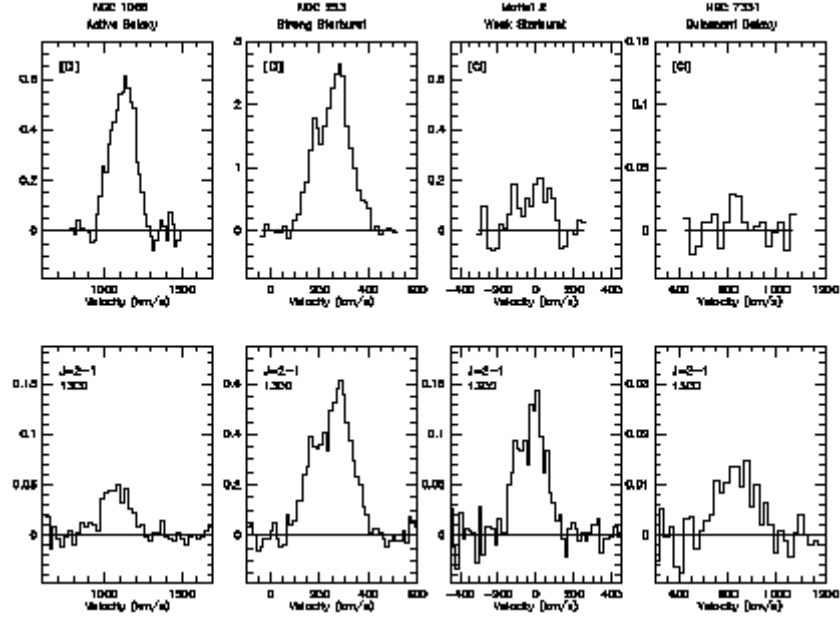


**Fig. 2.4:** 492-GHz [CI] and 220-GHz 13CO (2-1) spectra toward various galaxies (Israel and Baas 2002). The [CI] emission tends to be more intense with increasing galaxy activity.

It is of our great interest why such a trend is observed. The 10 arcsec beam of JCMT is not enough to study details of what happens in these regions. The distances to these galaxies are of order 1-10 Mpc, so 10 arcsec corresponds to 0.5-5 kpc. Without ACA, it would be impossible to scrutinize the origin of atomic carbon well, or to understand the difference between galaxies directly.

By observing both [CI] 1-0 and [CI] 2-1 transition of atomic carbon, we will be able to derive the spatial variation of physical parameters such as the gas temperature and atomic carbon density. By comparing CI and CO isotopomer lines ( $^{12}\text{CO}$ ,  $^{13}\text{CO}$ , ...), we will be able to derive the spatial variation of relative abundance of atomic carbon. Such studies will address to a question what the variety of galaxies actually means.

### a-4) Ultraluminous IR galaxies at Bands 8-10 line ratios of high-excitation lines.

These galaxies contain a lot of warm dust and gas at a temperature of order 100 K, which is heated by massive star formation or AGN activities, at their centers. Such gas can be observed with

high-excitation molecular lines. For such a purpose, ACA system will play a critical role in imaging performance. High-fidelity imaging with ALMA will lead to full understanding of the physics of this class of objects.

**a-5) Late-type stars at Bands 8-10: line ratios of high-excitation lines.**

The mass-loss from late-type stars is poorly understood. The circumstellar envelope made of mass-loss is important observational targets to understand the mass loss. Because envelope is warm or hot, we can observe the envelope with high frequency lines and with high spatial resolution with ALMA.

**a-6) Vega-like stars.**

Debris disk around the main-sequence stars are of our great interest, because it is related to star formation and planet formation. With ALMA, we will be able to survey such a disk as far as 100 pc, which makes reliable statistics possible. Imaging of two or more (submillimeter) bands will provide the vital information of the disk evolution and dispersal process.

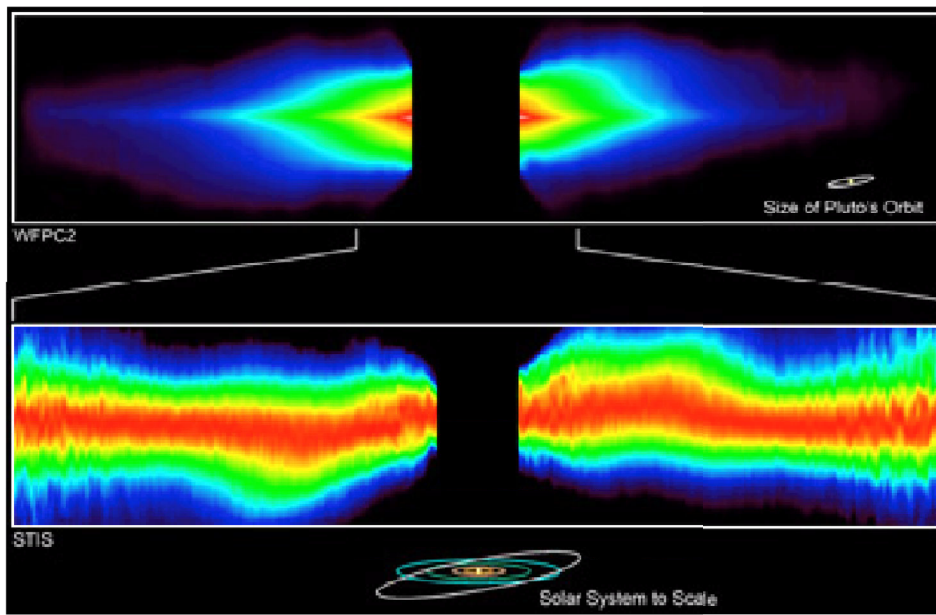


**Fig.2.5:** Beta Pic with the Hubble Space Telescope (Schultz, Heap, and NASA 1998)

## b) Importance of ACA at low frequencies

The ACA will be important also at low frequencies, because observers can obtain high signal-to-noise ratio more easily due to lower system noise temperatures. In low-J molecular lines, the angular size of the Galactic molecular cloud is large (due to lower critical densities), and the ACA system will be essential to derive the true intensity distribution.

### b-1) Fragmentation of the Galactic molecular cloud and the origin of IMF

The origin of the stellar initial mass function is one of the most important issues left for astronomy. Because the interstellar molecular cloud is known to be the site of star formation, its fragmentation is one of the promising candidates of the origin. For such a purpose, we need very high fidelity of the image of the molecular cloud. To entangle the excitation condition and optical depth, we will need to make multi-line comparison. Without ACA, it is impossible to address to such a problem.

These a few years, many young brown dwarfs (candidates) and isolated planets (candidates) have been found. Their origin is not clear. Detailed studies of the fine structure of the Galactic interstellar molecular cloud will provide a key to understand how they form.

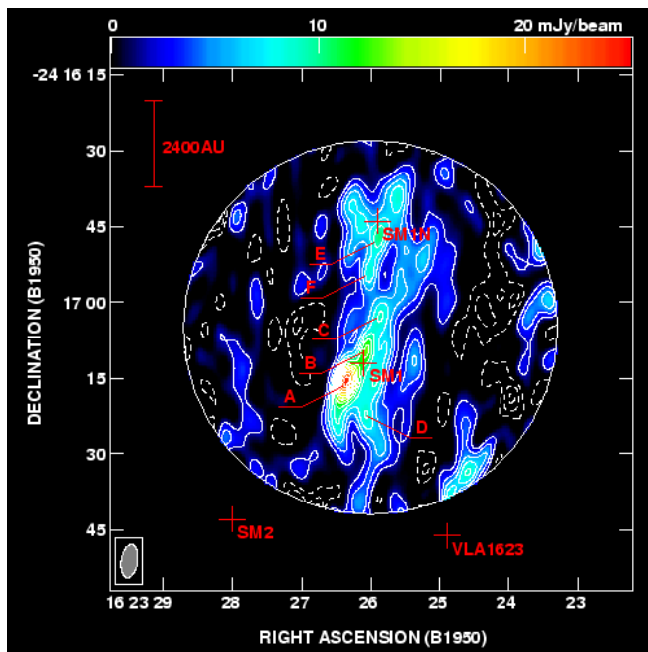


Fig. 2.6. 3mm dust continuum image obtained with the Nobeyama Millimeter Array (Kamazaki et al. 1991)

### b-2) Arm/interarm ratios of galaxies

The formation mechanism of the interstellar molecular cloud is one of the very important problems in astronomy. One of the proposed mechanisms is gas compression due to the spiral density wave in galaxies. Detailed studies of spiral density waves have been difficult for our Galaxy because of edge-on configuration, and also difficult for external galaxies because of limited angular resolution

and sensitivity of existing millimeter/submillimeter telescopes. With ALMA, we can study galactic density waves in detail enough to be compared with theoretical studies. ACA will play an essential role because the structure in arm/interarm may be overlooked in 12m interferometric observations only.

### b-3) SZ effect in Band 1

Sunyaev-Zeldvich effect is scattering of the cosmic microwave background radiation by the hot plasma in the cluster of galaxies, and is an effective way to measure the cosmological parameter, the Hubble constant. We need to compare X-ray image and radio images precisely. Currently, the uncertainty in radio measurements is the largest. ALMA will provide vital information regarding SZ effect, in particular at Band 1 due to very good sensitivity. With observations of SZ effect with the ACA system, we will be able to attack an important problem whether the universe is open or close.

It is also important to measure the fluctuations of the cosmic microwave background radiation at various angular scales to constraint cosmological models.

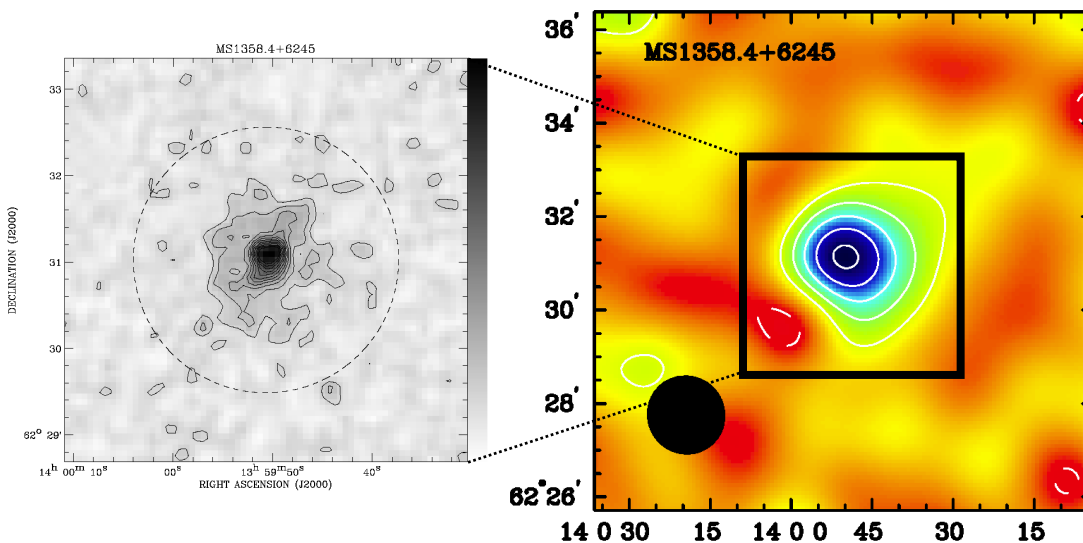


**Fig. 2.7:** Left X-ray image of hot plasma in the cluster of galaxy (Lewis et al. 1999). Right) Image of the SZ effect with millimeter interferometer (Grego et al. 2001).

#### **b-4) Polarization**

Magnetic fields play a very essential role in many astrophysical phenomena. Polarization measurements help us to understand the meaning of magnetic fields in astronomy. Because the magnetic field is ubiquitous in the interstellar medium, we need faithful information on various angular scales. Polarization of the dust continuum emission provides us with information on the direction of magnetic fields, both at lower and higher frequencies. Observations of Zeeman splitting of CCS (33.8, 45.4 GHz) and SO (30.0 GHz) (Shinnaga and Yamamoto 2000) will be a promising tracer to measure the strength of magnetic field, and will need the ACA system (Also, we will need reconsideration of the frequency range of Band 1).

#### **References**

- ALMA Science Advisory Committee, 2001, "Science Justification for the ALMA Enhancements".
- Dressler, A., Dickinson, M., Macchetto, Giavalisco, and NASA 1994, "Galaxies: Snapshots in Time," STScI-PRC1994-52c,  
HubbleSite, <http://hubblesite.org/newscenter/archive/1994/52/image/c>
- Grego, L., et al. 2001, "Galaxy Cluster Gas Mass Fractions from Sunyaev-Zeldovich Measurements: Constraints on  $\Omega_M$ ," ApJ 552, 2.
- Israel, F.P., and Baas, F. 2002, "Neutral Atomic Carbon in Centers of Galaxies," A&A 383, 82
- Kamazaki, T., Saito, M., Hirano, N., and Kawabe, R., 2001, "Millimeter-wave Interferometric Study of the  $\rho$  Ophiuchi A Region," ApJ 548, 278.
- Lewis, A.D., Ellingson, E., Morris, S.L., and Carlberg, R.G. 1999, "X-Ray Mass Estimates at  $z \sim 0.3$  for the Canadian Network for Observational Cosmology Cluster Sample," ApJ 517, 587
- McCaughrean, M., and O'Dell, C.R. 1995, "Hubble Space Telescope Spies Planetary Systems in the Making," STScI-PRC1995-45b,  
HubbleSite, <http://hubblesite.org/newscenter/archive/1995/45/image/b>
- Nakai, N., Kuno, N., Handa, T., and Sofue, Y., 1994, "Distribution and Dynamics of Molecular Gas in the Galaxy M51. I. Data and Spiral Structure", Publ. Astron. Soc. Japan 46, 527.
- Schultz, A., Heap, S., and NASA 1998, "Astronomers Have Found a New Twist in a Suspected Proto-Planetary Disk," PRC1998-03,  
HubbleSite, <http://hubblesite.org/newscenter/archive/1998/03/>
- Shinnaga, H., and Yamamoto, S. 2000, "Zeeman Effect on the Rotational levels of CCS and SO in the  $^3\Sigma^-$  Ground State," ApJ 544, 330.



# Science Requirements

Tetsuo Hasegawa and Koh-Ichiro Morita

## Revision History

2004-02-15: First Draft

## 3.1. General Requirements

### 3.1.1. Precise Imaging of Extended Objects

As described in **Chapter 1**, the major goal of introducing the ACA system is to enable ALMA to image extended objects with high precision and robustness. Here, an “extended” object means one that has a spatially extended structure with a size comparable with or larger than the beam size of the 12-m element antenna of the 64-element array.

The image precision can be expressed by the statistics of “fidelity”, which is defined as a pixel-by-pixel value of the true image brightness divided by the brightness difference between the true image and the image reconstructed from the observed data. It is foreseen that quantitative comparison of images taken in various wavelengths across the electromagnetic spectrum becomes a norm in the astrophysics in the ALMA era. To meet this need, we require that ALMA with the ACA system should routinely achieve a median fidelity of 20 or better in the portion of the image brighter than 1% of the peak, regardless the spatial structure of the source, if the image is taken in millimeter wave (frequency < 345 GHz) in an average observing condition. The similar level of fidelity should be achieved for submillimeter (frequency > 345 GHz) images taken in a fraction of observing time with favorable conditions.

This derives a further requirement that the following major factors need to be controlled well:

#### **UV coverage:**

The ACA should have a good UV coverage at the UV gap of the 64-element array so that the total UV coverage with the ACA and the 64-element array provide a good synthesized beam with low sidelobe level.

#### **Sensitivity**

Within a reasonable observing time, the sensitivity of the ACA at the *UV* gap should be comparable with that of the ALMA 64-element array around minimum baseline area.

**Calibration:**

In general, the calibration accuracies of the data taken with the ACA System should at least as good as those of the 64-element array data. This is true for the amplitude, phase, bandpass, baseline, polarization, and the shape of the primary beam. In addition, some of these calibration items are required to be of higher accuracy

**Scheduling:**

The ACA data should be taken in conditions for small phase and pointing errors. A clever dynamic scheduling is highly required for the ACA operation.

**3.1.2. Compatibility with the 64-element array data**

For the ACA System to contribute to the imaging capability of ALMA, it is required that the data from the ACA System is compatible with those from the 64-element array, so that the two datasets can be combined without difficulty. There are three aspects for which the compatibility is important, 1) the observing frequency, 2) spectral channels in spectroscopy, and 3) calibration. In the following we discuss the requirements in each of these aspects.

**Observing frequency**

In most of the scientific programs, the observing frequencies must be identical between the ACA system and the 64-element array. It will be most effective if we can equip the ACA system with the receiver frontends that cover the same frequency range as the 64-element array. The receiver frontend cryostat for the 64-element array has rooms for 10 receiver cartridges corresponding to 10 receiver bands. The current plan is that the bilateral project installs 4 receiver bands (Bands 3, 6, 7, 9) and Japan installs additional three bands (Bands 4, 8, 10) leaving rooms for two more cartridges to be installed later. It would be ideal to install the same set of bands also in the ACA receiver frontend in a compatible design.

**Spectral channels**

In spectral line observations, the spectro-correlators for the ACA System and the 64-element array must have a compatibility in that the central frequencies and the frequency response of individual spectral channels are close enough with each other.

**3.2. Specific Requirements****3.2.1. Sensitivity**

As we discussed in **chapter 2**, the ALMA observing programs that require data taken with the ACA System comprises no less than 25% in observing time. The ACA System is required to have a sufficient

sensitivity and observing speed to keep pace with the observations of this fraction of programs with the 64-element array.

From the sensitivity point of view, it is expected that ACA with twelve 7-m dishes can achieve the sensitivity that matches with that of the 64-element array at the  $uv$  distance of about 15 m, if ACA observes 4 times longer with the same system noise temperature and antenna gain (**Figure 3.1**). In the **Figure 3.1**, it is also indicated that the choice of packing ratio 1.25 and 7 m antenna diameter is appropriate one. In the same context, four dedicated 12-m antennas taking single-dish data most of the time is expected to achieve a sufficient sensitivity.

More realistic comparison requires us to take antenna configuration into account (Morita and Holdaway, 2004). **Figure 3.2 (a)** shows an example of the sensitivity comparison between the four single-dish 12-m antennas, ACA in one of the configurations being tried, and the most compact configuration of the 64-element array. Observing time of the ACA is 4 times longer than that of the 64-element array. **Figure 3.2 (b)**: Same plot for the case of the 64-element array configuration with almost 1 km maximum baseline. In this case Observing times for both of arrays are same. Although they are roughly comparable in sensitivity, the four 12-m dishes are less sensitive than the 64-element array.

The sensitivity for visibility gain measurement is shown in **Figure 3.3**. This is very important for pointing, amplitude, and phase calibrations. The figure indicates that the ACA System needs to spend more time in calibration to compensate for the smaller collecting area of the ACA dishes.

Thus it is important to take possible options listed below to recover the sensitivity or increase the observing speed of the ACA system:

#### **Antenna**

- Design the antenna optics to minimize the wavefront curvature loss because the 7-m antenna should have faster primary F ratio for close packing.

- Improve the surface accuracy for a higher gain in submillimeter wavelengths.

#### **Correlator**

- 3-bit correlation as standard to recover the sensitivity loss in 2-bit correlation.

#### **Calibration**

- Shorten the time required for calibrating 7-m antennas by using the four 12-m antennas in the interferometer to enhance the sensitivity.

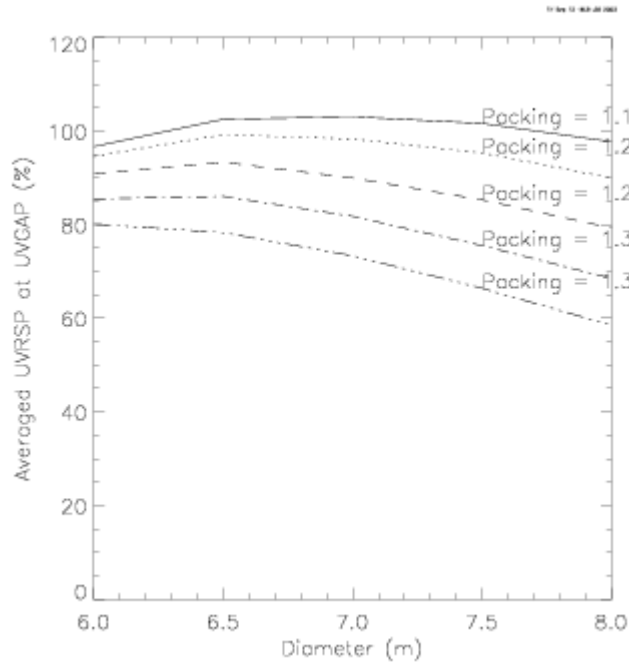


**Figure 3.1.** Averaged  $UV$  sensitivity at the  $UV$  gap as a function of diameter of ACA antennas with various packing ratio. Sensitivity scale is relative to the averaged  $UV$  sensitivity of the ALMA C1 array around shortest baselines.

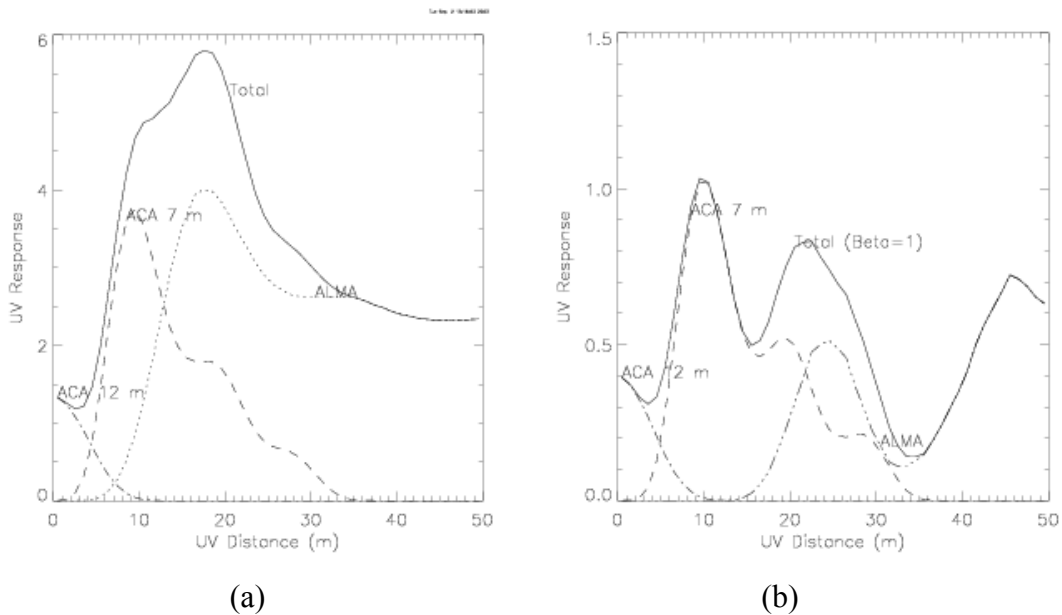


**Figure 3.2.**  $UV$  sensitivity profile of the ACA and the most compact configuration of the 64-element array. (a): The configuration of the 64-element array is the most compact one. Observing time of the ACA is 4 times longer than that of the 64-element array. (b): The case of the 64-element array configuration with almost 1 km maximum baseline. Observing times of both array are same.

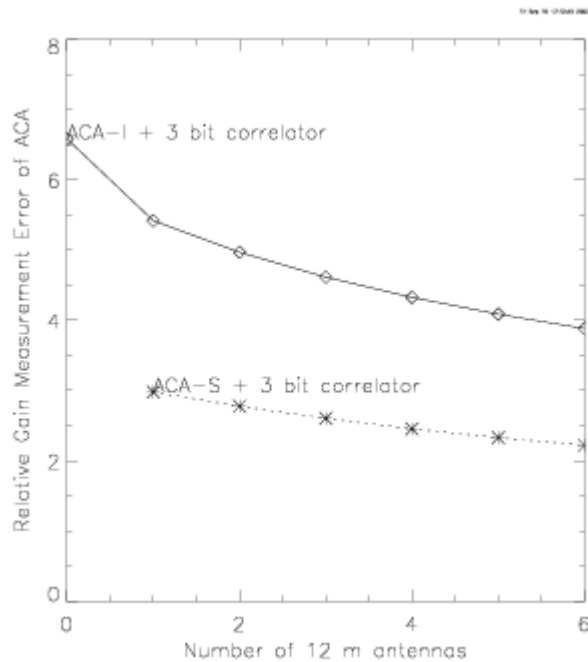


**Figure 3.3.** Relative calibration error (= [measurement noise]) of the ACA system as a function of number ACA 12 m. Relative error = 1 for the case of ALMA 64-element ACA-I: ACA 7 m dish For, ACA-S: ACA 12 m dish.

### 3.2.2. ACA configuration

The ACA configuration should be optimized with a careful consideration of the points discussed below.

#### Sampling of short $uv$ spacing

The configuration of the ACA is one of the keys in its design. It should enable the array an accurate sample of the short  $uv$  spacing (within a  $uv$  radius of about 15 m) with a sensitivity comparable with that of the 64-element array. Then the data should be combined with the data from the 64-element array to produce high-fidelity images of extended objects. The ACA configuration must be designed toward this goal.

Thanks to the simulation tools developed based on GILDAS and AIPS++ image reduction packages, it is possible for us to check how a given configuration performs in delivering high-fidelity images under various observing conditions (e.g., with various sets of pointing, phase, and beamshape errors and thermal noise; Tsutsumi et al., 2004). The simulations made so far indicates that the close packing ratio (the minimum distance between the antenna centers divided by the antenna diameter) of the 7-m antennas is one of the key parameter as shown in **Figure 3.4**, although making it smaller tends to contradict with the requirement for high precision of the main dish. A minimum distance smaller than the collision radius

of the antenna could be possible with a safety interlocking (Welch 1995), but the risk may be too high for a failure of the system that can cause a serious damage of the antenna in the long expected life of ALMA. A careful system design is needed, and a good starting point may be 1.25 without possible collision, the same value as the 12-m antennas

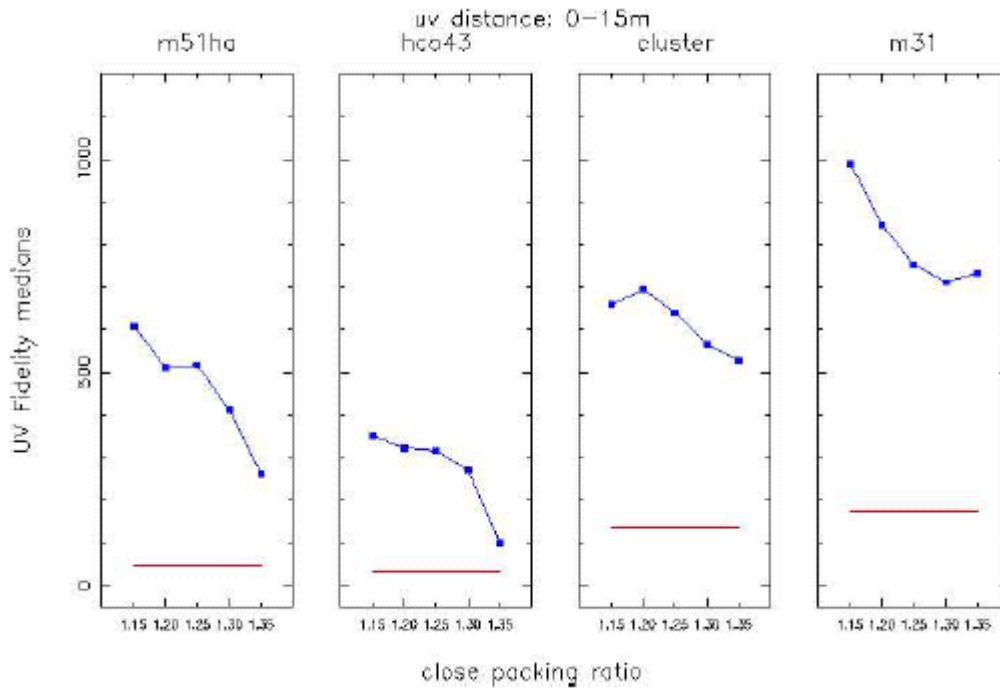


**Figure 3.4.** Comparison of fidelities in different close packing ratio.

### Sky coverage and observable HA range

Another important aspect of the ACA configuration design is the sky coverage, i.e., the declination range of the sky that can be observed with the array without too much shadowing. A related parameter is the hour angle (HA) range (as a function of declination of the source) over which the array can observe without too much shadowing.

In general, it would be ideal for the ACA to have the same sky coverage as the 64-element array in its compact configuration, because we can fulfill our main goal by combining the data from both arrays. The compact NS array configuration for the 64-element array can cover a declination range from about  $-85^\circ$  to  $+40^\circ$  with 55 antennas unshadowed although the HA coverages are very limited at both ends of the declination range

(J. Conway; <http://www.oso.chalmers.se/~jconway/ALMA/SIMULATIONS/SIM23/>).

However, ACA may be more susceptible to shadowing in observing low elevation sources, because a close-packing is required to sample short  $uv$  data and the number of element antennas is limited. It is

certain that a NS-elongated configuration is required for ACA to cover the sources with extreme declinations, in addition to the more round and compact configuration suited to observations of high-elevation sources. In designing the ACA configuration, it is important not to miss astronomically important and prominent objects near the declination limit. **Table 3.1** shows a list of such objects near the northern and southern limits of observation. We note that near the northern limit lie many objects important for science and for calibration. We should compromise the configuration to cover many of them if possible.

**Table 3.1.** Prominent objects near the observable declination limits

	declination (deg)	elevation at transit (deg)
Sources near the Southern limit		
Chamaeleon III dark cloud	-79	34
Chamaeleon II dark cloud	-77	36
Chamaeleon I dark cloud	-77	36
N84/SMC	-74	39
LMC-S	-71	42
N159S/LMC	-70	43
LMC-N	-69	44
Sources near the Northern limit		
M33	31	36
Cygnus Loop	32	35
S106	37	30
NGC 4151	39	28
GL 2591	40	27
MWC 349	41	26
M31	41	26
3C84	42	25
DR 21	42	25
BL Lac	42	25
N7027	42	25
M51	47	20

We should also consider the longer integration time (typically 4 times longer ) required for ACA to achieve the sensitivity comparable with the 64-element array. For example, an object that can be observed in mosaic by the 64-element array in 30 minutes near transit (HA ~15 min) requires 2 hours of observing with ACA (HA ~1 hour). Because the scientifically interesting sources tend to have an uneven distribution in RA, it would sometimes be required to (dynamically) allocate the observing time off the transit. This situation requires a large HA coverage by ACA. On the other hand, the larger offset from transit reduces the efficiency of observations because the atmospheric attenuation and phase fluctuation increase with higher airmass, reducing the relative weight of the data. Holdaway (1998) presented a set of simulation of the effective HA range as a function of declination based on the statistics of site testing data. Typically, hour angle limits of 2 – 3 hours (i.e., 4 – 6 hours of total observing) are possible without

increasing the system temperature too much.

### Support for a stand-alone observation

It has been noted that ACA can also serve as a stand-alone array in a compact configuration at any time for high frequency work (e.g., “Scientific Justification for the ALMA Enhancements” attached to the ASAC report, October 2001). For example, ACA yields an angular resolution of 1.5” at 900 GHz, similar to that provided by the compact configuration of the 64-element array at 230 GHz. Thus, images of low- and high-excitation lines could be compared on the same angular scale. Although this is not the main goal of the ACA System, care must be taken in designing the ACA configuration so that ACA should have a beam with reasonably low sidelobes to support such science.

### 3.2.3. Calibration

#### Pointing

Figure 3.5 shows the image fidelity medians as a function of ACA 7 m pointing errors in presence of ALMA 12 m pointing error of 0.6” at 850 GHz. When the pointing error of ALMA and ACA 12 m are 0.6”, the pointing error of ACA 7 m also significantly influences the image quality. Therefore, the relative pointing specification of ACA 7 m dish should be more tighten than that of ALMA 12 m dish.

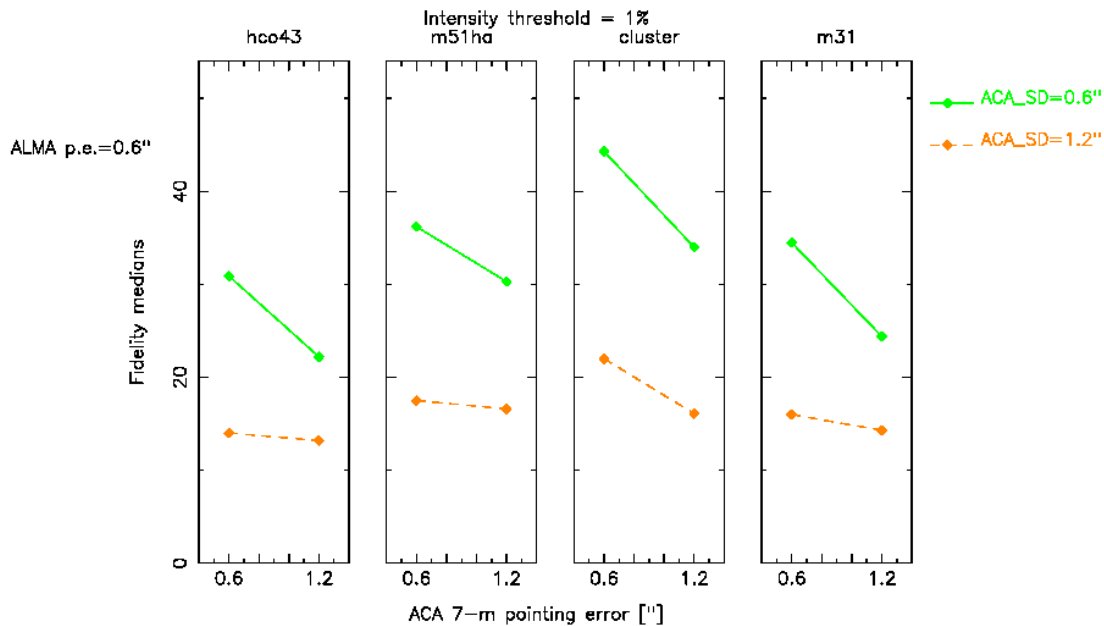


Figure 3.5. Image fidelity medians as a function of ACA 7 m pointing errors in presence of ALMA 12 m pointing error of 0.6” at 850 GHz. The green solid line: ACA 12 m single dish pointing error of 0.6”; the orange dashed line: for the ACA 12 m pointing error of 1.2”.



### Atmospheric phase calibration

Since the maximum baseline length of the ACA system will be less than 50 m, the atmospheric phase error is expected to be very small. At the observing frequency < 350 GHz, no special phase calibration method may not be needed under about 50 % site condition. At the frequency > 350GHz, atmospheric phase fluctuation often influences image quality. For the 90 % of site condition at 850 GHz, the ACA would not be improve image qualities of the wide field mosaic observations.

Minimum baseline length where the fast switching method is effective is given as

$$L = (v t_{cycle} / 2 + h\Delta\theta)$$

Where  $v$  is wind velocity at the phase screen height  $h$ ,  $t_{cycle}$  is the fast switching cycle time, and  $\Delta\theta$  is angular distance between a target source and a phase calibrator. Since typical wind velocity,  $v$  at phase screen height is expected to be faster than 10 m / s,  $t_{cycle}$  should be less than a few seconds to obtain  $L < 20$ -30 m. Therefore, the fast switching cannot be used to remove the residual phase error.

WVR method is considered only possible to calibrate the atmospheric phase error. However current specification of the WVR instrument for the ALMA is not enough for sub-millimeter observations.

**Table 3.2.** Image fidelity medians at intensity threshold of 1% at 230 GHz with typical systematic errors.

Model	Site condition	Median Fidelity (Intensity threshold 1 %)	
		ALMA+SD	ALMA+ACA
HCO43	No error	8	105
	25 %	8	44
	50 %	9	33
M51 Ha	No error	28	151
	25 %	22	46
	50 %	17	26
Cluster	No error	65	267
	25 %	64	88
	50 %	37	48
M31	No error	99	220
	25 %	88	71
	50 %	47	39

### Imaging performance under typical systematic errors

Table 3.2 and 3.3 shows the results of simulations including all the errors discussed above. The

parameters were chosen based on the ALMA specifications, which are 0.6 arcsec rms for pointing errors, 1 % (offset term) at 230 GHz and 3 % (offset and drift terms combined) at 850 GHz for amplitude errors. These results indicate that the almost same calibration specifications of the ACA system as those of the ALMA 64-element array are required to obtain high precision imaging.

**Table 3.3.** Same as Table 3.2 but at 850 GHz

Model	Site condition	Median Fidelity (Intensity threshold 1 %)	
		ALMA+SD	ALMA+ACA
HCO43	No error	8	105
	5 %	8	44
	10 %	9	33
M51 Ha	No error	29	156
	5 %	20	29
	10 %	17	18
Cluster	No error	63	255
	5 %	20	27
	10 %	22	29
M31	No error	99	222
	5 %	27	28
	10 %	24	27

### 3.2.4. Single-dish capability

As we discussed in Section 3.1, the four 12-m antennas in the ACA System is required to have good pointing and beam accuracy with an accurate amplitude calibration. In addition, these 12-m antennas should have an enhanced capability for single-dish data taking.

The accuracy of single-dish maps of extended radio continuum sources is seldom limited by the statistical noise from the receiver. This is because the observation is susceptible of systematic errors caused by the fluctuating atmospheric emission/absorption and variations of the receiver gain. Several studies have been made to remove this systematic effect (Holdaway, Owen, and Emerson 1995; Wright 2000; Welch 2003). Holdaway, Owen, and Emerson (1995) estimated the total power error made in subtracting the atmospheric emission for beam-switched and on-the-fly (OTF) continuum observations, based on the phase monitor data at Chajnantor. They found that, on the Chajnantor site at 230 GHz and 4 GHz bandwidth, switching on time scales of 1 second will usually increase the continuum total power noise by 50 %. If switching can be done on time scales of 0.2 second, the atmosphere will only rarely limit the

noise. Wright (2000) and Welch (2003) noted that the wide instantaneous bandwidth (8 GHz) of the ALMA receivers calls for unusually good gain stability of  $\sim 1 \times 10^{-4}$  over a timescale of  $\sim 1$  second for the gain variation not to dominate the error.

#### **Nutating subreflector**

If the extent of the source is not larger than a few beamwidths of the 12-m antenna, the most efficient way in measuring the total power flux is by beam switching with a nutating subreflector. The nutator should switch the beam at a speed of  $\sim 5$  Hz.

#### **On-the-fly mapping**

(to be added later)

#### **Polarization measurement**

(to be added later)

### **3.3. The ACA System in the early science observations**

In September 2002, the ALMA Science Advisory Committee (ASAC) made an assessment of the “ALMA early science”, in response to the charge from the ALMA Coordinating Committee (ACC). In the ASAC report submitted to the ACC in October 2002, a following recommendation was made among others: “The ASAC recommends having 1 antenna instrumented with total power mode capability for Early Science, if possible.”

The plan being considered at NAOJ can fulfill this requirement by making at least one 12-m antenna in the ACA System available for single-dish observations at the start of the Early Science Observations in Q3 2007. The antenna will be equipped with a nutating subreflector, and the signal from the backend subsystem can be fed to the Baseline Correlator via the optical fiber patch panel. The availability of the receiver bands is to be determined.

The capability of the ACA System grows rapidly with time. By Q3 2009, the ACA System with up to seven 7-m antennas and four 12-m antennas with a limited number of receiver bands will work as a part of the entire ALMA System, providing short baseline data to a good fraction of programs in the Early Science Operations. When ALMA starts full science operations in Q1 2012, the ACA System is ready for its full operation except that some antennas need to wait some more months for remaining cartridges to be installed.

## References

- Holdaway, M. A., Owen, F. N., and Emerson, D. T., 1995, MMA Memo 137, "Removal of Atmospheric Emission from Total Power Continuum Observations".
- Morita, K.-I. And Holdaway, M. A., ALMA Memo in preparation, "UV Sensitivity Reponse of the Atacama Compact Array"
- Thompson, A. R., Moran, J. M., and Swenson, Jr., G. W., 2001, "Interferometry and Synthesis in Radio Astronomy", 2<sup>nd</sup> ed. (John Wiley & Sons, Inc.).
- Tsutsumi, T., Morita, K.-I., Hasegawa, T., and Pety, J., 2004, ALMA Memo in preparation, "Imaging Simulations for the Atacama Compact Array".
- Welch, W. J., 1995, MMA Memo 134, "Some Comments on Sampling, Antenna Spacings, and uniform Aperture Illumination".
- Welch, W. J., 2003, ALMA Memo 454, "Total Power Observing with the ALMA Antennas".
- Wright, M., 2000, ALMA Memo 289.1, "Atmospheric Noise in Single Dish Observations".
- Wright, M., 2003, ALMA Memo 450, "Heterogeneous Imaging with the ALMA Compact Array"

# Operations of the ACA System

Tetsuo Hasegawa & Koh-Ichiro Morita

## Revision History

2004-02-14: First Draft Version

## **4.1. Joint Operation of ALMA Including the ACA System**

The ACA System works as a subsystem of ALMA, and its main role is to provide the short spacing and total power data to be combined with the data taken with the 64-element array for a fraction of the science programs executed with ALMA. For this purpose, the ACA System needs to be operated in harmony with the other parts of the entire ALMA system. This is best done by including the ACA System in the entire ALMA system as a single observatory jointly operated by North America, Europe, and Japan. We assume in the rest of this document that a joint operation scheme is taken.

The operation plan described in this Chapter should be consistent with that of the 64-element array.

## **4.2. Coordinated Science Operations of the 64-element Array and the ACA System**

To fulfill the scientific role of the ACA System in ALMA, its operations should be coordinated with those of the 64-element array throughout all stages of the science operations of ALMA, from preparation of proposal to data taking, pipeline data processing, and data archive. Basic observing process for the ACA system is same as the 64-element array. We summarize the issues related to the ACA science operation.

### **4.2.1. Observing Proposal for the ALMA 64 element array and the ACA.**

In the Phase 1 observing process, a proposer will be required to prepare and to submit a Proposal to perform a set of observations and it will be reviews by a program review committee. Whether a

Proposal should include information about use of the ACA is TBD. Only information about requested the wide field imaging quality may be sufficient in this phase.

At beginning of the Phase 2 process, PIs with newly approved programs will be required to complete their Projects which will be created from their Proposal. The Project consists of the approved part of the Proposal and additional information including a list of requested configuration of the 64-element array and the ACA. Typical Projects for imaging will be planned to use the 64-element array only or the 64-element array and the ACA system. Request for concurrent observation of the 64-element array and the ACA would be limited to time critical observations of solar system objects and other time variable sources. There may be a small fraction of Proposals to use the ACA system only; There is only one such a project in DRSP.

#### 4.2.2. Observation modes in the ACA system

Ordinary modes are

- to use the 7 m antennas for interferometric observations.
- to use the 12 m antennas for single dish observations
- to use both of the 7 m antennas and the 12 m antennas for calibrations.

Typical observing sequence of the ACA system is shown in Figure 4.1.

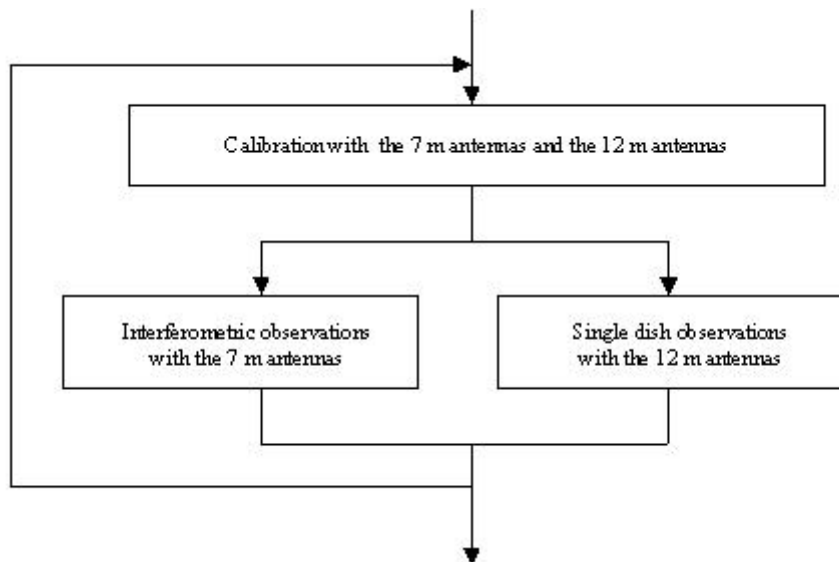


**Figure 4.1.** Typical Observing Sequence of the ACA system.

It is also possible to use both of the 7 m antennas and the 12 m antennas for interferometric observations.

Observing data, which includes cross correlation and auto correlation from all antennas of the ACA system shall be provided from the ACA to ALMA pipeline system and ALMA archive system. Visibilities of baselines between the ACA system and the 64-element array shall be not taken due to the reason mentioned in Chapter 3.

### **4.2.3. Observing Preparation**

Based on the sensitivity estimate in Chapter 2, it is expected that the ACA System has an observing speed about 25 % of that of the 64-element array and can provide data for up to about 25 % (in the 64-element array observing time) of the scientific projects executed with ALMA. The practical value of this fraction needs to be defined by the ALMA observatory based on the actual status of the instrument, observing conditions, etc., and should be known to the prospective users of ALMA.

The above discussion indicates that an observing project that requires the ACA data needs four times more observing time for the ACA System than that for the 64-element array to equalize the signal-to-noise ratio over the  $uv$  plane. In the actual situation, the signal-to-noise ratio should vary with the structure of the observed source (i.e., its power spectrum with spatial frequency).

The need for the ACA data is not always easy to assess for scientists planning observations with ALMA, and the ALMA Regional Centers (ARCs) should provide a tool (a simple simulator, for example) and advices to help their decision. . Screening process of proposals should have a mechanism to assure that an appropriate fraction of accepted proposals require ACA observations.

The same tool (Observing Tool) will be used in ALMA 64-element array and ACA observations. The Observing Tool shall provide observers with a suggestion whether the ACA will be used or not.

### **4.2.4. Scheduling**

For a majority of the observing programs, data taking with the ACA System does not need to be concurrent with that with the 64-element array. Exceptions include time critical observations of solar system objects and other time variable sources.

In general, short term scheduling (<1 week) of the ACA need not to be connected with that of the ALMA 64-element array. Exceptions are time-critical projects (e.g., highly variable objects) that require a tightly coordinated scheduling of the two arrays to ensure concurrent observations.

Making the best use of the excellent observing conditions at the ALMA site is important also for the

ACA system, dynamic scheduling is highly needed for the ACA. The same decision algorithm as the one for the 64-element array may be used.

The scheduling for long time scale (reconfiguration cycle of the 64-element array) should be loosely coordinated with that of the 64-element array, so that the epochs of data taking with the two arrays shall not be too separate.

#### **4.2.5. Pipeline and Archive**

ALMA pipeline system and ALMA archive system shall be able to handle observing data from the ACA correlator, which includes cross correlation and auto correlation from all antennas of the ACA system.

For the case of science programs which need both the ALMA 64-element array and ACA, the pipeline shall create images from data obtained in the ALMA 64-element array and the ACA, i.e., 12 m interferometric data, 7 m interferometric data, and 12 m single-dish data.

Furthermore, pipeline should be done by extracting the appropriate data taken previously, from the archive. For example, if 64-element observation is made before ACA observation, pipeline only using the 64-element data is done at the time of 64-element observation, and then pipeline using the ACA data being obtained and 64-element data from archive at the time of ACA observations.

### **4.3. Operation and Maintenance of the ACA System at AOS and OSF**

#### **4.3.1. Basic Concept**

In according to the basic model for the operations and maintenance of the ALMA 64-element array, the ACA will be operated and maintained by Array Operations Site (AOS), Operation Support Facility (OSF), Central Office, ALMA Regional Centers (ARCs). A summary of the functions at each locations is included in Table.

AOS -Chajnantor	Antenna reconfiguration Instrument module exchange Security of site
OSF -San Pedro	Array scheduling + operations Quick-look reduction



Maintenance + repair antennas  
Maintenance + repair instrumentation  
Administration, Safety

Central Office  
- Santiago  
Standard pipeline reduction, quality assessment  
Archive production  
Business functions  
Science offices

ARCs -NA, EU, JP Proposal handling  
User support for proposals, data reduction  
Host of archive copy, archival research support

#### **4.3.2. Operating at the AOS**

The only antenna transport teams of ALMA will be present on a daily basis at the AOS as same as ALMA 64-element array operation. The teams will check status of the antenna, the antenna, all the equipment and instrumentation installed on the antenna, regularly. Every 6 - 12 months, they will replace oil and grease of the antenna drive system. If they find an instrumentation or an equipment with malfunction, they will exchange the module or bring back to OSF.

#### **4.3.3. Operating at the OSF**

The antenna will be moved to OSF for major maintenance every 2 years. The antenna arriving from the AOS will be earmarked either for repair or overhaul. After the engineers test the fundamental performance (Surface accuracy measurements / AZ-EL axis crossing angle) of the antenna at the OSF, the antenna will be shipped to AOS.

Basic maintenance for all equipment of the ACA system except for the correlator will be done at the OSF. Because of modularity and reliability, only simple maintenance should be needed for the OSF engineers and technician. If a band-4, band-8, or band-10 cartridge has a serious trouble, the cartridge will be shipped to NAO-J for fixing the trouble.

# ACA System Design

S. Iguchi, K.-I. Morita ed.

## Revision History

2004-02-17: First draft

## 5.1. Introduction

In this chapter, we give a design concept of the ACA system. Detailed descriptions of each subsystem are written in other chapters.

There are two important aspects which need to be considered in designing the ACA system as follows:

- To have the optimum performance for the requested scientific goals.
- For a smooth and effective operation as a sub array of the ALMA, the design of each ACA subsystem should be identical or at least compatible to that of the ALMA 64-element array.

As described in the previous chapters, we have two main scientific goals for the ACA, which are to provide high fidelity imaging and wide field imaging capability to the ALMA. The ACA will be mainly operated with the ALMA 64-element array to accomplish such scientific projects

Sensitivity of the ACA is always a key point for the above scientific goals. We shall not be able to obtain precise calibration without sufficient sensitivity. For this reason, we will adopt 3 bit correlation architecture for the ACA correlator. This architecture reduces the quantization loss and increases the sensitivity by 9 %. This specification is different from that the ALMA 64 element array.

High antenna performance is very important for the ACA. In particular, the performance at sub-millimeter wavelengths is critical, because primary beam width of 12 m antennas is less than 10 arcsec at these wavelengths and demands for wide field imaging is very high. Therefore, the specifications of the ACA antennas are determined to be better than that of the 64-element array.

## 5.2. Calibration Method

### 5.2.1. Calibration requirements

The calibration goal to the ACA summarized in Table 5.1 should be consistent with those to the ALMA 64-element array (Butler et al. 2003). However, since the calibration sensitivity of the ACA system is about one fourth of that of the 64-element array for same integration time, if we use astronomical calibrators, we have to carefully choose the calibrator and integration time to obtain almost same calibration accuracy. Several issues are written in the following subsections.

Pointing	2.0 arcsec (blind); 0.6 arcsec (offset)
Primary Beam	6% in power out to 10% point
Amplitude	1% (<345GHz) and 3 % (>345GHz)
Antenna Location	65 $\mu$ m
Geometric Delay	5 fsec systematic
Atmospheric Delay	10 fsec systematic
Antenna Delay	7 fsec systematic; 30 fsec random
Electronic Delay	7 fsec systematic; 30 fsecs random
Bandpass	1000:1 in most cases; 10000:1 in a few select cases
Polarization	0.1 % in amplitude; 6 deg in position angle
Sideband Gain Ratio	0.1 %

Table 5.1. Calibration Requirements.

### 5.2.2. Pointing

Basic strategy of the pointing calibration is same as the 64-element array. The first step of the pointing calibration is to remove the systematic pointing errors by using the pointing model. Frequent (i.e. every 15 - 30 minutes) offset pointing calibrations during astronomical observation will be conducted, to remove local deviations from the pointing model.

The specification of offset pointing accuracy for the ACA 7m antenna is 0.6 arcsec for the case of the calibrator 4 deg away from the target source which is 2 times further than for the case of the ALMA 12 m. Therefore, pointing calibrators with about 3 times stronger flux than those used for the 64 element array will be available for the offset pointing calibrations and so that it is possible to achieve the same pointing accuracy as that of the 64 element array.

### **5.2.3. Phase Calibration**

For phase drifts or atmospheric phase fluctuation the standard switching method using reference calibrators with every 15 to 30 min interval will be used. As mentioned in Chapter 3, the fast switching cannot be used to remove the residual phase error. WVR method is considered only possible to calibrate the atmospheric phase error. However current specification of the WVR instrument for the ALMA is not enough for sub-millimeter observations. At the moment, current design plan does not include WVR systems for the ACA system.

### **5.2.4. Single Dish Calibration**

Because single-dish observing is in total power, albeit it switched against, for example, blank sky, there are extraordinary demands for instrumental gain stability. In addition, the extra, variable emission from the sky comes in directly, and tends to mask the much weaker (by perhaps 4 orders of magnitude) astronomical emission. This is in contrast to interferometry, which of course by the use of cross-correlation rather than self-correlation, is relatively immune to these disadvantages.

Astronomical calibration in single-dish mode has to be on a dish-by-dish basis; calibration sources need to be detectable with adequate signal-to-noise ratio by one single dish of the array. This is again in contrast to interferometric astronomical calibration measurements, in which the large collecting area of the entire array can contribute to the signal-to-noise ratio achievable in calibrating individual dishes of the array.

Polarization calibration of single dish observations has its own problems. At mm-waves, polarization measurements are conventionally made with a "widget" in front of the receiver feed. This "widget" introduces changes in the polarization response of the receiver – for example a rotating grid and screen combination can continuously rotate the incident plane of linear polarization. The astronomical polarization is then detected by synchronous changes in total power intensity through the receiver as the sense of polarization changes. The ALMA may indeed have to provide such "widgets" for each of the antennas. However, the complexity and potential unreliability of such a device could be avoided if it were shown possible to measure polarization reliably, in single-dish mode, by cross-correlation of the signal from orthogonally polarized feeds.

### **5.2.5. Cross Calibration between the ACA system and the 64-element array**

Cross calibration between the ACA 7 m array, the ACA 12 m single dishes, and the 64-element array is very important to obtain high fidelity images. Using overlapping regions in UV plane, amplitude gains of the ACA interferometric data, the ACA total power data, and the 64-element interferometric data can be cross-checked.

### 5.3. Configuration

From several studies of the ACA imaging (ALMA memo 398, ALMA memo 374), there are several important parameters related to the array configuration

- The minimum baseline length should be short as possible.
- The compactness of UV distribution is very important.
- Sidelobe level of the synthesized beam of the ACA should be low as possible.

Specifications of the ACA 7m array configuration design derived from the above points are follows:

- The close packing ratio of the ACA 7m antennas is set to be 1.25 and the minimum baseline length will be designed to be 8.75 m.
- The maximum baseline length in the E-W direction will be less than 40 m. In the N-S direction, it should be determined by considering the shadowing effect.
- Antenna positions will be randomized as possible and the UV sampling distribution will have a tapered profile.

A conceptual design is showed in Figure 5.1 (a).

To avoid severe shadowing effect, an elongation in the N-S direction is needed in the actual design. The ratio is TBD. Furthermore, to cover requested declination range, two different configurations will be provided, both of which will share the same 6 pads in the EW direction. Therefore, the total number of pads for the ACA 7 m array is 18. Figure 5.1 (b) shows an example of such a configuration for low elevation observations.

Distance between the ACA 7 m array and the ACA 12 m antennas should be close as possible to realize accurate calibrations or/and good performance of the ACA heterogeneous mode (ALMA memo 450, Wright).

Several configuration designs are investigated by imaging simulations. Table 5.2 shows median image fidelity with four different ACA configurations, which are “spiral” in Figure 5.1, “iram” in ALMA memo 398, “mw2003” in ALMA memo 450, and “ring” (typical circular array). It is clear that addition of the ACA greatly improve the imaging performance in general. Difference among four types of configurations depends on the source structure, but it is not significant. Therefore, for detailed design of pad positions, it would be more important to take account of actual operation (shadowing, transporter accessibility, etc), although rough design come from study of imaging performance.

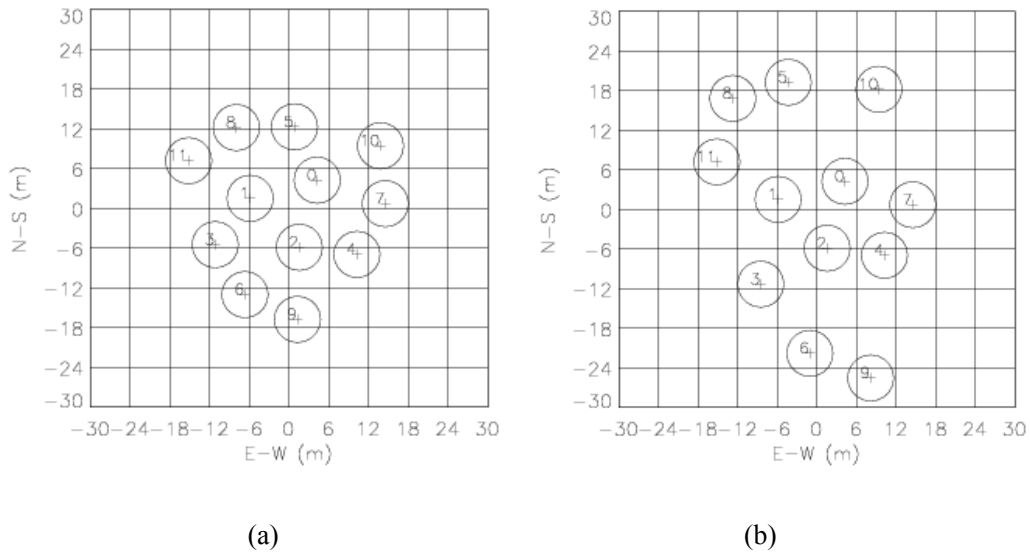


Figure 5.1. An example of the ACA array design concept. (a) is the configuration for high elevation observations. (b) is for low elevation observations.

model	ACA config.	Intensity threshold											
		0.30%			1%			3%			10%		
		AS	AAS	$\frac{AAS}{AS}$	AS	AAS	$\frac{AAS}{AS}$	AS	AAS	$\frac{AAS}{AS}$	AS	AAS	$\frac{AAS}{AS}$
M51ha	iram	5	54	11.0	28	148	5.3	51	206	4.0	102	300	2.9
	ring	5	15	3.0	28	44	1.6	51	85	1.7	102	180	1.8
	spiral	5	53	10.8	28	151	5.4	51	213	4.2	102	296	2.9
	mw2003	5	53	10.8	28	127	4.5	51	171	3.4	102	269	2.6
HCO43	iram	6	66	10.9	8	110	14.6	21	156	7.3	20	168	8.3
	ring	6	13	2.1	8	17	2.3	21	42	2.0	20	52	2.6
	spiral	6	62	10.1	8	105	14.0	21	164	7.6	20	180	8.9
	mw2003	6	44	7.3	8	73	9.7	21	107	5.0	20	113	5.6
cluster	iram	46	195	4.3	65	250	3.9	95	300	3.2	186	408	2.2
	ring	46	161	3.5	65	224	3.5	95	292	3.1	186	403	2.2
	spiral	46	207	4.5	65	267	4.1	95	311	3.3	186	416	2.2
	mw2003	46	186	4.1	65	235	3.6	95	285	3.0	186	379	2.0
M31	iram	85	184	2.2	99	221	2.2	117	273	2.3	138	338	2.5
	ring	85	180	2.1	99	219	2.2	117	264	2.3	138	333	2.4
	spiral	85	184	2.2	99	220	2.2	117	278	2.4	138	331	2.4
	mw2003	85	183	2.2	99	221	2.2	117	276	2.4	138	333	2.4

Table 5.2. Median image fidelity with different ACA configuration designs.

## 5.4. Antennas

### 5.4.1. Basic Concept and Specifications

The ACA antenna system consists of four 12-m antennas and twelve 7-m antennas. The former one, equipped with a nutator, is used as a single dish and interferometric calibration for the 7-m antennas. The basic concept and specifications of these antennas are similar to the 12-m antennas of the 64-element array as summarized in Table 5.3.

<b>Common Specifications for 12m and 7m Antennas</b>	
Configuration	Elevation-over-azimuth mount, Cassegrain focus
Frequency Range	35 GHz to 950 GHz
Precision Performance Conditions	Nighttime: wind 9 m/s Daytime: wind 6 m/s and sun from any angle
Pointing Accuracy, rms	0.6 arcsec (offset, 4 deg in position and 15 min time) 2.0 arcsec (absolute)
Path Length Stability	10 $\mu$ m rms (offset, 4 deg in position and 15 min time)
Solar Observing	Allowed
Transportability	Transportable on the same vehicle as the 64-element array
<b>Specifications for the 12-m antennas</b>	
Reflector Surface Accuracy	25 $\mu$ m rms, spec
Fast motion Capability (1)	6 deg/sec 24 deg/sec/sec in Az 3 deg/sec 12 deg/sec/sec in El
Geometrical blockage	3%
Edge Taper	-12dB
<b>Specifications for the 7-m antennas</b>	
Close Packing	1.25 dish diameters
Reflector Surface Accuracy	20 $\mu$ m rms, spec
Fast Motion Capability	6 deg/sec 6 deg/sec/sec in Az 3 deg/sec 3 deg/sec/sec in El
Geometrical blockage	4%
Edge Taper	-12dB

Table 5.3. Antenna specifications.

- (1) Fast motion capability of the 12-m antenna highly depends on OTF requirements and details are under investigation (see Chapter 3).

## **5.4.2. Common design issues for the ACA antennas**

### **5.4.2.1. Pointing Accuracy**

A required pointing accuracy in "offset" pointing mode (calibrator 4 degrees away every 15 minutes of time) are 0.6 arcsec RSS for offset pointing, 2.0 arcsec RSS for absolute pointing. At night this accuracy is to be achieved in a wind of 9.0 m/s, which is the 90th percentile wind for nighttime (2000 hours to 0800 hours) observing. During the day this accuracy is to be achieved for any orientation of solar illumination in a wind of 6 m/s.

The ratio of 0.6 arcsec to primary beam width of the 7-m antenna is smaller than that of the 12-m antenna. However, imaging simulations (Tsutsumi et al. 2004) shows that high frequency mosaics benefit from better pointing accuracy and therefore the pointing accuracy of the 7-m antenna is set to be 0.6 arcsec.

### **5.4.2.2. Path length stability**

Phase errors caused by variations in the propagation path length through the antenna can be rapidly or slowly varying. Fast phase changes are primarily caused by the wind and the peak path length variation in a 9.0 m/s wind must be no more than 10  $\mu\text{m}$ . Slow phase changes are primarily due to variations in the temperature of the antenna and the goal is to keep these phase errors small enough so that the residual errors after an astronomical phase calibration every 3 minutes are small enough to allow observations at 900 GHz. The severer residual phase error residual is required for the ACA array because of shorter baselines than the main array.

### **5.4.2.3. Low antenna noise**

Contributions to system noise from the antenna, due to such mechanisms as scattering of ground noise into the feed and resistive loss of reflector surfaces, will be minimized as much as possible without compromising the surface accuracy and pointing requirements. Design features to be considered to achieve this goal include supporting the subreflector support legs close to the edge of the reflector and shaping the underside of the support legs to reduce ground pickup. Geometrical blockage will not exceed 4.0% and resistive loss of any reflective surface will not exceed 1.0% at frequencies up to 950 GHz. This argument does not apply to the 7m antenna design because there is a large Cassegrain hole in the center required by the receiver optics. 4 % Geometrical blockage will be accepted for 7m antennas.

### **5.4.2.4. Transportability**

Both the 12-m and 7-m antennas must have the interface to the transporter used for the 64-element array.



### **5.4.3. Specific Design Issues for the 12-m Antenna**

#### **5.4.3.1. Reflector surface accuracy**

The surface accuracy specifications is 25 mm RSS for the 12-m antennas including the subreflector contributions. The 25  $\mu\text{m}$  surfaces will provide antenna surface efficiencies at 300GHz /900 GHz of 90%/40%. At night this accuracy is to be achieved in a wind of 9 m/s, which is approximately the 90<sup>th</sup> percentile wind for nighttime (2000 hours to 0800 hours) observing. During the day this accuracy is to be achieved for any orientation of solar illumination in a wind of 6 m/s. During the day the focus can be calibrated astronomically every 30 minutes.

#### **5.4.3.2. Fast motion capability**

On-the-fly mapping, which is major observing mode for the ACA 12-m antennas requires high performance of the fast motion capability. In this mode the antenna will scan at a rate of up to 0.5 deg/sec across a large object, several or many beamwidths in size, and then turn around as rapidly as possible and scan back across the source in the opposite direction. A maximum acceleration of 12 deg/sec/sec is required for the turn around. As the antenna tracks across the source it is not necessary for the position at any time to be precisely a precommanded position; it is sufficient to simply know where the antenna is actually pointing and all antennas need not point precisely at the same position.

### **5.4.4. Specific design issues for the 7-m antenna**

#### **5.4.4.1. Optics**

A different optics is required to meet the specification of close packing ratio as discussed by Baars (2000, ALMA memo 339). We note that the minimum collision radius is not always limited by the distance between the El axis to the top of the subreflector structure as Baars (2000) assumed. In case of low f/D ratio, the collision radius is determined by the distance to the edge of the main dish. ACA design strategy in the present plan is not to minimize the collision radius, but to maximize the focal ratio as close to as 0.4 in order to reduce the aberration loss and cross polarization. This requirement comes from the fact that the off-axis distance of the feed of the 7-m antennas is relatively farther from the Az axis compared with the 12-m antennas because of shorter equivalent focal distance.

#### **5.4.4.2. Close packing**

In the ACA array the antennas must be placed close together to fill the gap of  $uv$  coverage taken with the 64-element array and single dish antennas. It shall be possible to place the antennas with their azimuth axis within 8.75 m (1.25 D) of each other without any possibility of the antennas hitting each other, no matter what the relative orientation of the two antennas.

#### **5.4.4.3. Surface accuracy**

The surface accuracy goal is the hard specification is 20 micrometers RSS, including the subreflector contributions. The 20 micron surfaces will provide antenna surface efficiencies at 300GHz /900 GHz of 96%/66%. Performance condition is same as that for the 12-m antenna.

#### **5.4.4.4. Fast motion capability**

Only on-the-fly interferometric mosaicing mode requires high fast motion capability of the 7-m antenna, because fast switching will be not used for the ACA system

On-the-fly interferometric mosaicing with 7m antennas requires interferometry data to be taken while the antenna is continuously scanning across the source. It is expected that the antenna velocity will be only 0.05 deg/sec but in this case all 7m antennas must point to the same position at the same time to within 1 arcsec rms. Consequently, 7m antennas are not required to have the fast motion capability as well as 12m antennas.

#### **5.4.4.5. Base**

7m antennas will have its own optimized mount base, which is compatible with the foundation the 12m antennas. It is, however, optimized to comply with the 7m antenna design and is different from that of the 12m antenna.

#### **5.4.4.6. Receiver cabin**

A receiver cabin will be provided at the Cassegrain focus. The same dimensions and interface as the main 12m will be provided for 7m antennas with possible minor modifications.

#### **5.4.4.7. Calibration instruments**

A nutator is not installed on the 7-m antennas since they are not used as a single dish in astronomical observations. The WVR also may not be needed for the 7-m antennas because the phase degradation for such short baselines often cannot be improved using the WVR. An optical guidescope and a holography system of the 7-m antennas will be smaller than those for the 64-element array.

## 5.5. Front End Subsystem

The ACA front end system will be designed basing upon compatibility with the ALMA front end system. The cartridges for 10 bands can be inserted in the system as well as a room for WVR. For the 12-m antenna, the receiver cabin, cryogenics, and optics are all fully compatible with the 64-element array according to the ALMA ICD standards. For the 7-m antenna, the cryogenics, power supply system, and mechanical structure for attachment of the front end system will be the same as those of the 12-m antenna, while the angles of the offset mirrors in room-temperature and cooled optics need to be corrected.

## 5.6. Local Oscillators

### 5.6.1. Basic Guideline

The important guideline for the LO system related to the Japanese deliverables including the ACA System is to satisfy interface conditions with the ALMA 64-element array and to minimize impacts on both baseline ALMA project and Japanese participation plan.

We have been developing photonic LO system with an aim to realize a direct photonic LO up to 950GHz (Band 10 receivers) [ALMA memo 449 (Sekimoto et al.), ALMA memo 435 (Ishiguro et al.) and ALMA memo 399 (Noguchi et al.)]. However, current technology of the “Direct Photonic” LO is premature for installation to ALMA. Therefore, we propose the “Photonic Hybrid” option which meets the requirement for initial installation to ALMA and could be simply modified to “Direct Photonic” LO in the future.

Since the low-frequency local oscillator reference system is strongly related to the ALMA computing control, it will be manufactured to have full compatibility with the 64-element array according to ALMA ICD standards.

### 5.6.2. Photonic LO Developments

Development of photonic LO system has been conducted at NAOJ in collaborations with NTT Laboratories and the University of Electro-Communications (UEC). One of the motivation for the photonic LO developments is that it can greatly simplify the LO system in ALMA (Payne et al., 2002). However, there has been a major concern in the photonic LO about the degradation of the SIS mixer noise performances. In order to study basic properties of photomixers, a W-band waveguide photomixer was fabricated using the Uni-Travelling Carrier Photo Diode (UTC-PD,

Ishibashi 1997). The UTC photomixer could generate 2 mW with a laser power of about 100mW (Ueda 2003a). The noise performance of the SIS mixer pumped by this photomixer was compared with that by a conventional Gunn LO. The degradation on noise performance was negligible in the frequency range of 98-105GHz and very small outside this range (Ueda 2003b).

The millimeter-wave spectroscopic observations of CS (J=2-1) were carried out toward the high-mass star-forming region W51(H<sub>2</sub>O) using the Nobeyama 45-m radio telescope and it was demonstrated that the photonic LO is very useful in astronomical observations (Takano 2003). The laser system used in these observations was an optical comb generator (Yamamoto 2002).

The most difficult requirement for the ALMA LO is to generate sufficient (>100 microwatt) power up to 950GHz (Band 10). To evaluate the high frequency performance of UTC-PD, a free-space photonic emitter with a log-periodic antenna was developed and the performance was measured with Fourier Transform Spectrometer (FTS) for 100 – 800GHz (Hirata 2002). The measured power decreases proportional to  $f^{-4}$  above 400GHz and the estimated power at 800GHz is about 10 microwatt.

### 5.6.3. “Photonic Hybrid” LO

There are three methods to generate 1<sup>st</sup> LO signals at each antenna.

- 1) “Photonic Direct” method
- 2) “Photonic Hybrid” method
- 3) “Photonic Reference” method

The baseline ALMA has adopted the “Photonic Reference” method in which the photomixer output is used only for phase-locking the Warm Multiplier Assembly (WMA) (see Fig. 5.2 upper panel). In this case the photomixer does not require high output power. In the “Photonic Direct” method, all the LO signals are generated by photomixing the optical beatnotes for all frequency bands. No frequency multiplications are necessary after the photomixers and the phase error or phase noise is not amplified through the multiplication processes. This merit provides the great advantage for the interferometry at submillimeter wavelengths. The “Photonic Direct” method is the simplest method and greatly reduces the complexity in the LO system and save the cost. With the existing photomixers based on the UTC-PD, it is possible to realize the “Photonic Direct” method up to Band 4. However, at this moment, it is difficult to generate sufficient power for Bands 5 to 10 with the “Photonic Direct” method.

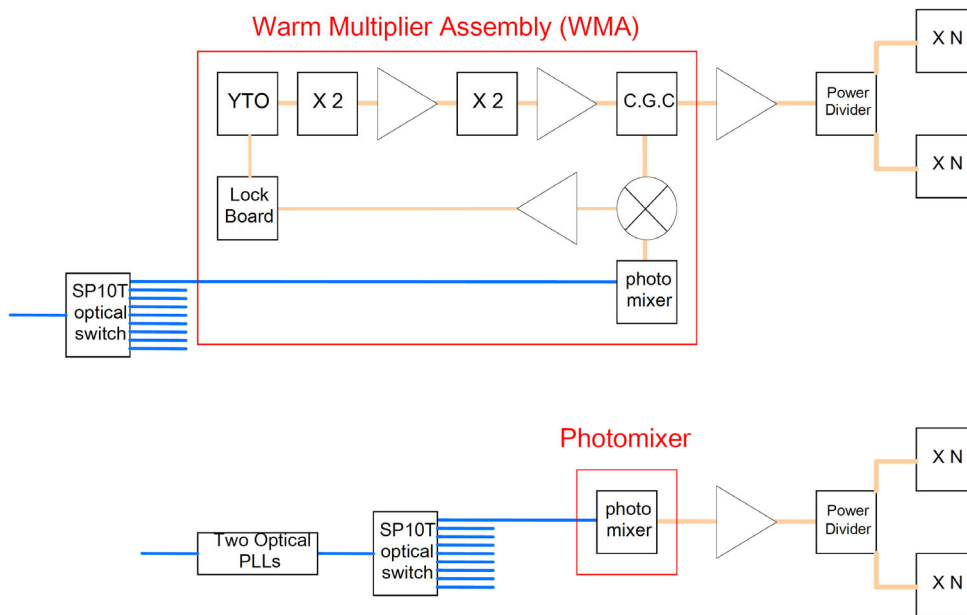


Figure 5.2 Comparison of a Warm Multiplier Assembly (WMA) and a single photomixer.

Since the cost of a single photomixer is much less than that of WMA, the “Photonic Hybrid” can eliminate a large fraction of electronics components and save the cost. Secondly, the large number of frequency multiplications especially for Band 10 LO in the baseline design may cause serious problems in phase noise and phase stability. Considering the above mentioned points, NAOJ has been proposing to adopt “Photonic Hybrid” option (Ishiguro 2002) in the 1<sup>st</sup> LO. In the proposed “Photonic Hybrid” LO, the outputs from photomixers are fed into mixers directly for band 4. For Bands 8 and 10, photomixer outputs ranging from 81GHz to 125GHz are used to drive power amplifiers and then frequency multipliers to obtain final LO signals. Because of the power limitation by Stimulated Brillouin Scattering in the long optical fiber, optical amplifier is required to feed enough power to photomixers. Phase stability of optical amplifier is not well known and may cause phase drift because it is outside the loop of round-trip phase correction. Another problem in this configuration is that it is difficult to incorporate fringe tracking at each antenna.

The alternative way to realize fringe-tracking function with high-power optical signal at each antenna is shown in Fig. 5.3. In this scheme, fringe tracking or frequency switching can be done by using DDS (Direct Digital Synthesizer) in PLL (Phase Lock Loop) control of one of the slave lasers and it is possible to meet the interface requirement with the baseline ALMA. Two slave lasers can be located in the same temperature-controlled and vibration-dumped box to minimize the differential effects between the two lasers. Total output power of ~100mW is expected. The proposed two-laser system at each antenna is basically compatible with the central LO system in the baseline

design. Therefore, it is possible to use the same central LO system not only in the baseline ALMA but also in the ACA System. At each antenna only one two-laser system is required for all frequency bands and thus it will eliminate a very large number of electronic components and save the cost correspondingly. In principle, “Photonic Hybrid” LO can coexist with “Photonic Reference” LO at each antenna.

Fig. 5.4 shows an implementation plan of the “Photonic Hybrid” LO compatible with the “Photonic Reference” LO. The central LO system should support 80 antennas and 6 sub-arrays instead of 64 and 4 sub-arrays, respectively. In the NAOJ proposal, antenna-based LO system includes a Two Optical PLL system (Fig. 5.3) followed by a single photomixer and corresponding power amplifiers/multipliers (Fig. 5.2 lower panel). The central LO part could be the same as the baseline design.

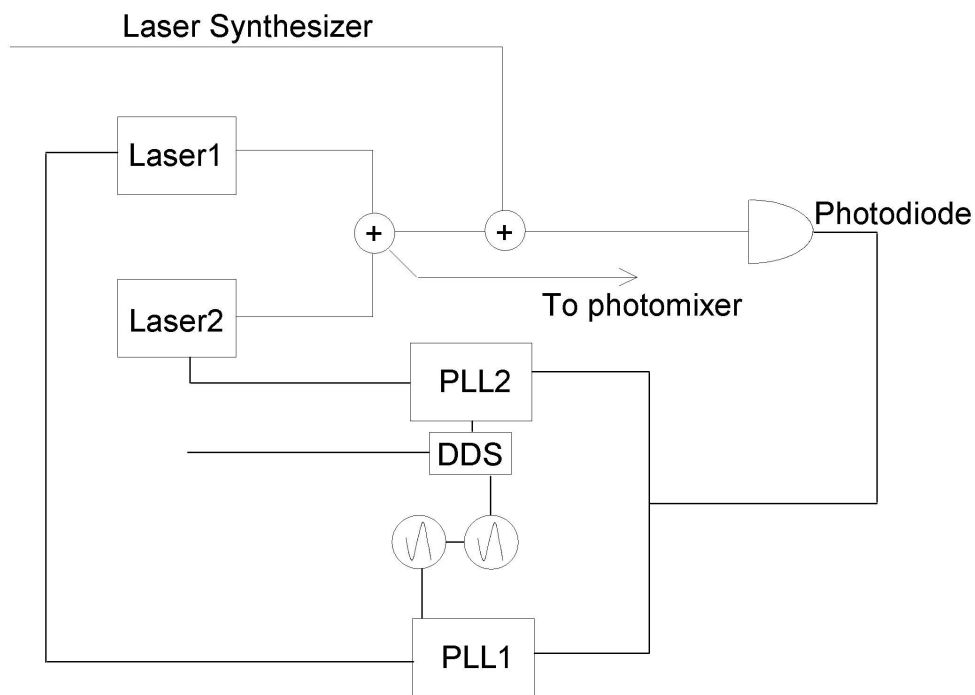


Figure 5.3 Schematic diagram of the Two Optical PLLs. The Optical PLLs. Optical reference signals are amplified with a capability of fringe tracking and phase switching.

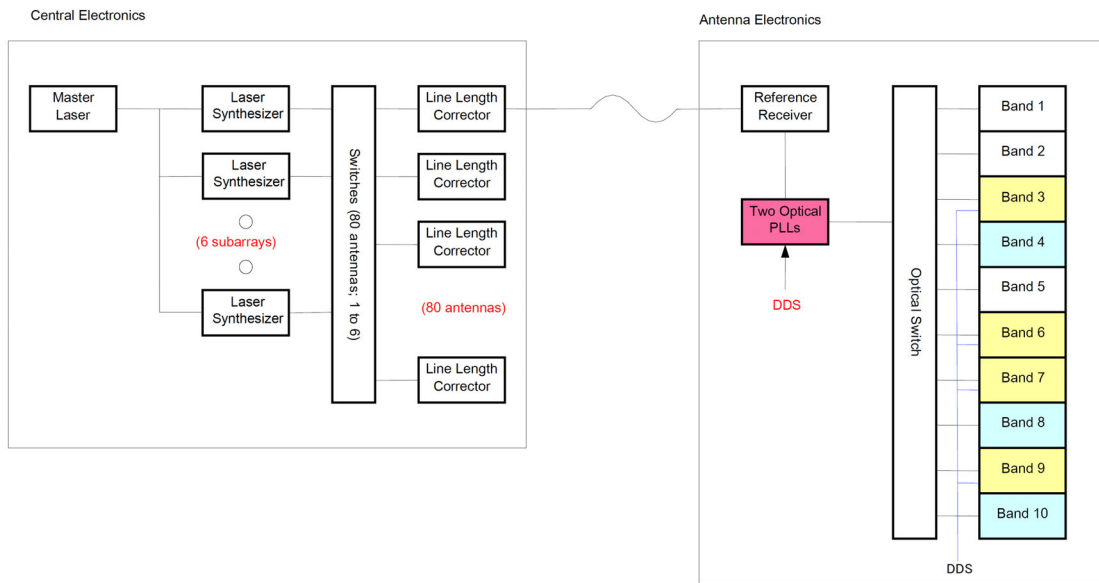


Figure 5.4 Antenna based LO system in the case of a combination of a single photomixer and WMA.

The performances of a “Photonic Hybrid” LO consisting of a laser system, a W-band photomixer, a W-band power amplifier, and frequency multipliers was demonstrated to be sufficiently powerful to pump an SIS mixer at 490 GHz (Sekimoto 2003). The noise temperature measured at 490 GHz was 135 K, which was comparable with that pumped by Gunn oscillator and multipliers. A plan for the “Photonic Hybrid” in the case of Band 8 cartridge is shown in Fig. 5.5.

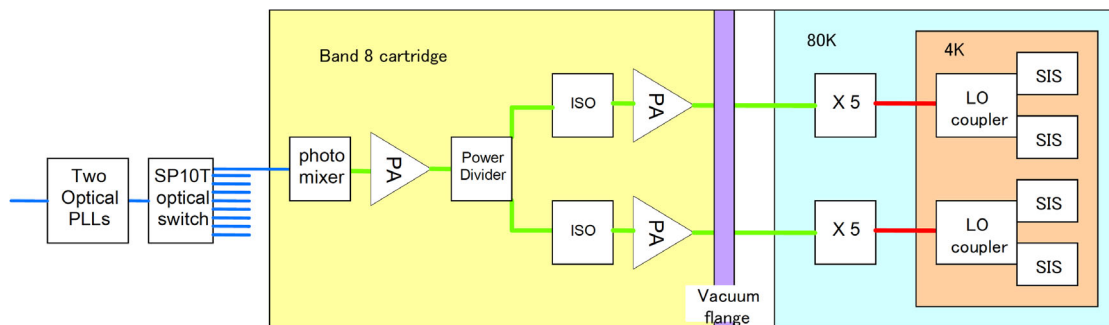


Figure 5.5 A plan for the Photonic Hybrid” LO in the case of Band 8 cartridge.

### 5.6.4. Master Laser

As a prototype of the master laser for ALMA, a new acetylene-stabilized laser is being developed in collaboration with UEC. We have developed an extended cavity diode laser (ECLD) stabilized on

a saturated absorption line of an acetylene molecule in the 1.5 micrometers region (Nakagawa 2001). This acetylene-stabilized laser has very good long term stability ( $\sim 4 \times 10^{-12} t^{-1/2}$ ) and satisfies most of the requirement for the ALMA master laser. NRAO photonics group visited Japan to make a preliminary test of the ALMA line length correction system using the old version of UEC laser (D'Addario 2003). The measurement set an upper limit on the delay variation in the stabilized path of about 70 fsec over 1 hour. However, the measurement with 25 km optical fiber was limited by the dithering output of the laser. UEC has developed a new laser with dither-free output which is expected to meet the ALMA specifications.

### **5.6.5. Compatibility Issues**

There are some compatibility issues in the current "Photonic Hybrid" design.

(1) In the current design of the ALMA central electronics, the Laser Synthesizer covers up to 140GHz (Shilue 2003). This is not enough to drive a photomixer for the Band 4 which requires the laser beatnotes up to 151GHz. This could be solved by adding another set of Photomixer and Harmonic Mixer for 129GHz to 151GHz inside the Laser Synthesizer unit. Addition of two Laser Synthesizer units is required to increase the number of subarrays from 4 to 6.

(2) The estimated size of the Two Optical PLLs is about 400Wx 400Dx 100H. The power supply unit should be separated with the Optical PLLs because of the vibrational problems. The estimated size of the power supply unit is about 400Wx400Dx300H which has enough space to install bias circuits for the Front End mixers and amplifiers. We need the space of 400H in total in the receiver rack at each antenna.

## **5.7. Backend Subsystem**

### **5.7.1. Basic concept and System block diagram**

The signal processing from the intermediate frequency (IF) outputs of the ACA Front End to the digital inputs of the ACA correlator is described in this Backend section. The ACA Backend consists of the following four parts :

- 1) IF Downconverter
- 2) Digitizer
- 3) Sampler clock module
- 4) Fiber Optic Data Transmission System (VPB and WDM)

The analog signals from the active front end at each ACA antenna will pass through an IF selector switch within the front end package and then into the IF Downconverter. The Downconverter put out eight sets of analog signals with 2-GHz bandwidth to 4Gsps AD Converters. Sampler clock module



supplies the necessary clock signals to the digitizer and the Data Transmission System( DTS ). Eight sets of 4Gsp/s 3-bit digital signals are sent to DTS, which will carry the digital signals from the antennas to the ACA correlator located in the central electronics building. The system block diagram of the Backend system shown in Fig.5.6. is the same as that of the 64-element array system.

### 5.7.2. Compatibility/Difference

IF Down converter, Digitizer, and Data Transmission System of ACA are all compatible with those of the ALMA 64-element array according to the ALMA interface control document (ICD) standards. All the modules of the ACA backend are presented in Fig.5.7. are the same hardware and software(control) interface as those of the 64-array system. Especially we will use the same back-plane between the Digitizers and DTS Transceivers as that of the 64-element array. It will allow us to make the complete compatibility with the card level. In addition, we propose to use the same type of patch panel as that of the 64-element array in the identical room of the central electronics building because of the side-by-side data acquisition experiments with 64-element array and ACA. It will be important to adopt the identical frame organization of the digital data in the DTS.

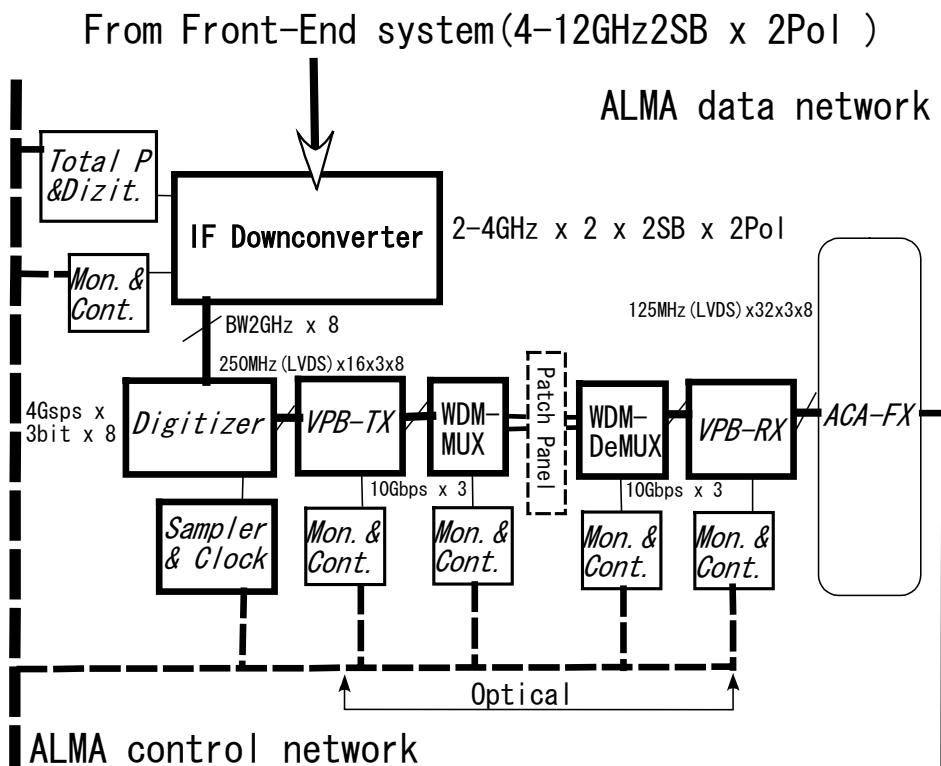


Figure 5.6. System block diagram of ACA BE (TBD).

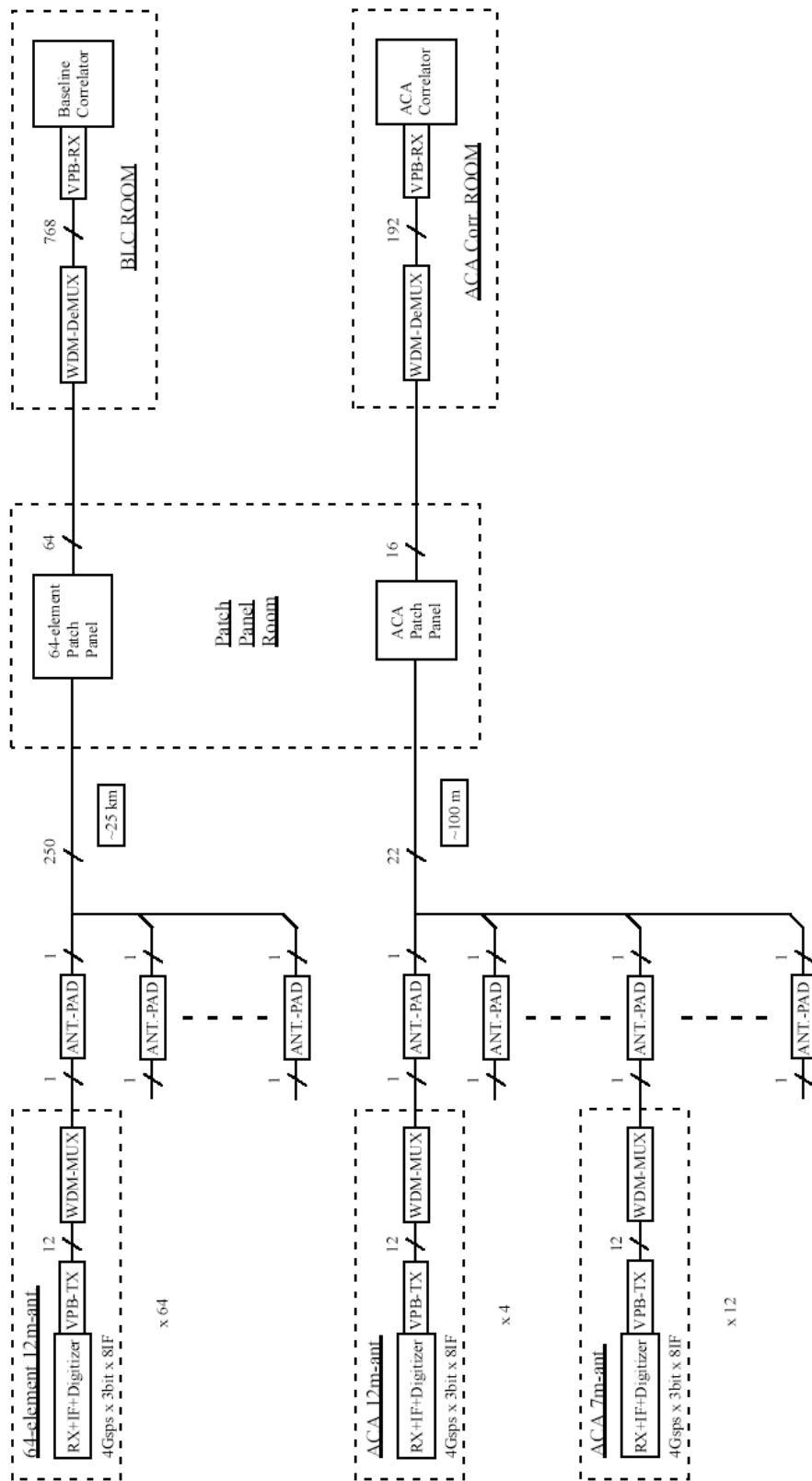


Figure 5.7. Block diagram of ACA and 64-element array Backend system

## 5.8. Correlator

### 5.8.1. Basic Concept and Specifications

The scientific requirement of ALMA correlator is high flexibility and high sensitivity. The ACA correlator has an enhanced spectroscopic capability that enables a flexible allocation of frequency resolution and the widest bandwidth. The correlator supports both a simultaneous operation of the ACA interferometric observations (with twelve 7-m antennas) and single-dish observations (with four 12-m antennas), and a 16-element interferometric observations. One more important point is high sensitivity. The loss of sensitivity caused by quantization of the signal should be minimized. Thus the ACA correlator supports more than 3-bit correlation, recovering 9 % in sensitivity relative to the baseline correlator( BLC ), for which 2-bit correlation is standard. This is a great compensating advantage for the smaller collecting area of the ACA antennas to assure that the ACA system can provide the single-dish and short-baseline data for the ALMA science programs whenever necessary. The detailed specifications of the ACA correlator are summarized in Table 5.3.

### 5.8.2. Compatibility/Difference

ACA-FX correlator satisfies all of the ASAC requirements for ALMA second generation correlator (2001) as shown in Table 5.4, and most of the science cases are covered as BLC and enhanced BLC does. The ACA FX correlator system could easily put out raw spectral visibility data to ALMA data archive system with the same channelization over each 2-GHz baseband as that of BLC/eBLC, because the FX correlator system rearrange the frequency channels of spectral visibility data at Correlator Out Interface in the ACA correlator data processor as shown in Figure 5.8. Thus there could be no extra-load for ALMA data network and archive system compared to BLC/eBLC. All the control data will be received at the ACA correlator control computer and the ACA spectral visibility data will be sent to the ALMA archive system according to the same format as the BLC/eBLC data. However, the following points are the differences between the ACA-FX correlator and BLC/eBLC;

- 1) Shape and width of the instrumental profile for each frequency channel,
- 2) Signal to noise ratio for the same integration time and frequency resolution,

First, as for 1), the shape of the instrumental profile at each frequency channel is proportional square of sinc-function though that of XF correlators is a sinc-function(see *Interferometry and Synthesis in Radio Astronomy*, 2<sup>nd</sup> edition, Lecture 4, Table4-1). However, the ACA-FX correlator has internally 512 x 1024 frequency-channel data over 2-GHz bandwidth with uniform 3.8kHz resolution just after the correlation calculation. Thus we could synthesize a similar shape and width of the instrumental profile in case that the frequency resolution of BLC/eBLC is low enough compared to 3.8 kHz.

Functions of both weighted integration after correlation and/or convolution of weighting function for time-serial data are possible in the ACA-FX correlator. In case of 8-channel averaging(  $3.8 \times 8 = 30.4$  kHz ), relative difference of the shape of the instrumental profile of FX to XF is less than 6% and it will be smaller in case of more averaging channels of FX.

Second, there is a difference of signal-to-noise ratio (SNR) for a unit integration time and frequency resolution between ACA FX and BLC/eBLC. One reason of the difference is the number of correlation bit mentioned in the above specifications. The other is a difference of relative density of lag measurements for FX and XF type correlators (see *Interferometry and Synthesis in Radio Astronomy*, 2<sup>nd</sup> edition, Lecture 4, Figure 4-9 ). The relative density of lag measurements for FX is low compared with that of XF correlator. There are two different types of method to compensate the SNR loss of FX. One is the segmentation overlapping as discussed in *Synthesis Imaging in Radio Astronomy II* ( Section 4, 5-7 ). The other one is the channel averaging as discussed in ALMA memo No.350( Okumura et al. 2001 ). The ACA-FX applies the latter method because the former one is largely affected to the correlator hardware size. In a simple case of uniform weighting functions of a XF-type correlator with 2-bit correlation and a FX correlator with 3-bit correlation, relative SNR of BLC/eBLC to ACA-FX is 13% with 3.8-kHz resolution. However, frequency-channel averaging of FX decreases the relative SNR ; the cases with more than 15.2-kHz resolution have no relative SNR loss of FX and the SNR gain is about 9% with more than 486.4-kHz resolution. In case that the ACA visibility data are combined with the 64-element visibility data, SNR of ACA visibility data should be equalize that of the 64-element data by the longer total observing time than the 64-element array. Therefore we should take the above SNR difference between ACA-FX and BLC/eBLC into account to obtain the same SNR data of ACA as the 64-element array.

Table 5.4. Specifications of the ACA Correlator

Specifications		Remarks
Number of antennas	16	
Number of correlations	120	
Bandwidth per baseband	2 GHz	2 GHz x 8 Basebands per baseline; Input = 4 Gsp/s x 3 bits
Input clock frequency	125 MHz	
Correlation functions	cross + auto	
180-degree phase switching	yes	
Image band rejection (90-degree switching)	yes	
delay compensation	yes	
Highest frequency resolution	3.8 kHz	Without a reduction of the total bandwidth
Correlation: Number of bits	3 bits	
Maximum number of frequency channels per baseband per baseline	4096 channels	
Integration time	1 msec (auto) 16 msec (cross)	
Sub-array	2	Supports single-dish mode and ACA interferometry simultaneously
Polarimetry	yes	not to reduce the total bandwidth and/or number of channel
VLBI phase-up mode	yes	

Connector



Block Diagram

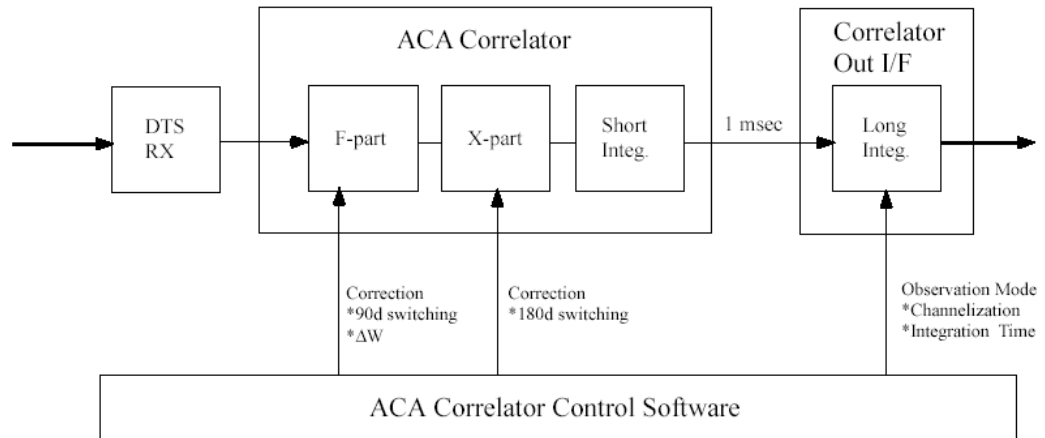


Figure 5.8. Conceptual block diagram of ACA-FX (TBD).

## 5.9. Computing

The ACA will be operated by the ALMA software system together with the 64-elements array. Following functions for the ACA operation are needed to be added to the ALMA software system.

- a) Monitor and control each device on the ACA antennas.
- b) Control the ACA correlator and acquire the data from the correlator.
- c) Dynamic scheduling function for the ACA and the 64-element array.
- d) Calibration and imaging functions for heterogeneous interferometric data.
- e) Observing preparation

### 5.9.1. Monitor and control each device on the ACA antennas

Although the interface of the ACA system will be compatible with the 64-element array, the ACA system will need software for the ACA specific hardware and ACA specific functionalities. It is needed to develop portions of the monitor and control software specific to the ACA system.

### 5.9.2. Control the ACA correlator and acquire the data from the correlator

On the basis of the correlator software for the (enhanced) baseline correlator, the software suitable to the hardware of the ACA correlator will be developed. The data output format must be compatible with that of (enhanced) baseline correlator (VOTable format and XML header, logging and error format).

### 5.9.3. Dynamic scheduling function for the ACA and the 64-element array

The ALMA dynamic scheduler is basically designed to have a functionality of treating subarrays. The ACA will be used as two subarrays (7-m antennas and 12-m antennas). It will be troublesome if the ACA observations is done long after the 64-element observations (the observer will want to publish the data without the ACA data). Therefore, the scheduler is needed to allocate the 64-element observations and the ACA observations as close as practical.

### 5.9.4. Calibration and imaging functions for heterogeneous interferometric data

For the hardware and functionaliteis specific to the ACA system, we need softwares for telescope calibration of the ACA system. The calibration strategy is the same as that to the 64-element array. Imaging of heterogeneous interferometric data in the pipeline and offlinesoftware needs appropriate treatment of different diameters of the element antennas (7 m and 12 m). This development is very essential for the ACA system.

The frequency of the pipeline operations will be increased by 25%, because 25% of all the programs use the ACA system and we need to pipeline again by using both of the 64-element data and the ACA data when ready. The pipeline hardware for the ACA system will be prepared separately, and can be used for pipelines for the ACA only data. It should be determined how pipeline hardware from Japan is incorporated into the overall pipeline system.

### **5.9.5. Observing preparation**

The observing tool is needed to be able to specify the ACA specific observing parameters. It is needed to supply the relevant simulator to the ACA system.

### **5.9.6. Data rate and the archive**

The current data rate used in the computing IPT is 60 MB/sec peak and 6 MB/sec average. The peak data rate consists of 40 MB/sec visibilities and 20 MB/sec images, while the average data rate consists of 4 MB/sec visibilities and 2 MB/sec images. In 2003 July, Science IPT recommended the data rate should be increased to 72 MB/sec peak and 7.2 MB/sec average. The visibility data rates are proportional to the number of baselines. The 64-element array has 2016 baselines, while the ACA system has 120 baselines. We propose to use the values recommended by the Science IPT, and divide the total data rate depending on the number of baselines: 94% is to be used for 64-element array and 6% is to be used for the ACA system consisting of 12 7-m antennas and 4 12-m antennas, if both operate simultaneously. Our plan is that the ACA correlator will be operated so that the data rate will not exceed 4.3 MB/s peak and 0.43 MB/s average.

The archive system which covers the increase in the data rate due to the ACA system (0.43 MB/s) and the temporary archive is to be prepared by Japan.

### **5.9.7. Development plan**

All functions mentioned above will be developed by cooperation between ALMA-J computing team and the computing IPT of the bilateral project and added to the ALMA software system currently developed for the 64-element array. This development will keep pace with that of the bilateral plan: releases will be made 6 monthly, and Incremental Critical Design Review will be done yearly for Phase 1 (-2007). It will also follow the decisions already made in the bilateral ALMA computing development.



## **5.10. Site Development**

### **5.10.1 Infrastructure at the AOS**

#### *Antenna foundations,*

4 for the 12 m antennas and 18 for the 7 m antennas will be distributed over an 80 m x 80 m area close to the compact configuration and the AOS building. The 22 foundations will be exclusively for the ACA system, but will be compatible to those of the bilateral project.

#### *Necessary infrastructure associated to the above antenna foundations,:*

Such as roads and electrical/optical connections among the pads and from the pads to the control building.

#### *Expansion of the AOS building for the ACA correlator:*

Space for ACA correlator and electronic staging. We presume the patch panel room and the LO reference rack room can consolidate those for both the BLC and the ACA correlator.

#### *Enhancement of electrical power:*

It covers extra power requirements due to the Japanese participation (1.6 MW max.).

### **5.10.2. Infrastructure at the OSF**

#### *An antenna assembly hall and an additional test pad:*

The assembly hall can be temporary if the ACA antennas can utilize the assembly hall for the baseline project for maintenance in the operations phase. The additional test pad is for assembly and testing of the ACA antennas.

#### *Expansion of the OSF building:*

For receiver assembly, operations, and maintenance of the instruments realized by the Japanese participation (e.g., labs and storage areas).

#### *Expansion of space for human activities :*

Offices, meeting rooms, and dorms etc.

#### *Contractors' camp area for the ACA system*

#### *Enhancement of electrical power:*

It covers extra power requirements due to the Japanese participation.

### **5.10.2 Array location**

Central location of the ACA system shall be determined considering following requirements:

#### ***Local topography***

General topographic constraints for the ALMA compact configuration.

#### ***Distance to the AOS buildings***

Because of the severe pressure on construction costs, it is preferable to reduce the length of trenches, fibers and cables by installing the ACA system close to the AOS buildings.

To reduce possible disturbance by the buildings and associated activities, however, the ACA system should not locate too close to the AOS buildings.

#### ***Distance to the ALMA compact configuration***

Closer is better for the following purposes:

- accurate relative intensity calibration between the ACA system and the 64-elements array,
- efficient holography measurements combined with the 64-elements array.

The ACA system should not be too close to the ALMA compact configuration so that the civil works related to the ACA system will not have severe impacts on the 64-elements array.

- Provided that the wind dominantly blows west-east, it is generally recommended to align the ACA system and the compact configuration in the north-south direction.
- Future operational flexibility of the ACA system increases if a number of pads surrounds the ACA pads and pad sharing is within the scope.

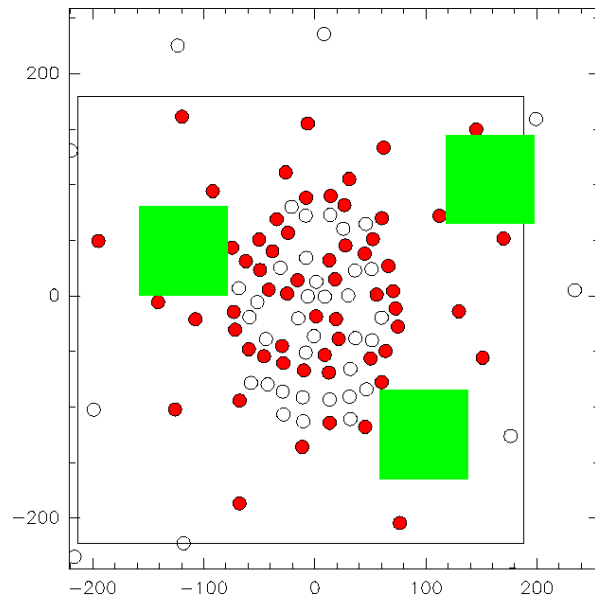


Figure 5.9. Candidate locations of 80 m x 80 m areas (green squares) spared for the ACA system. Coordinates are offset from the compact configuration in meters.

## References

- Baars, J, in ALMA memo series, No.339
- Burton 2001, in **ALMA memo series**, No.342
- Cornwell, T.J., Holdaway, M., Uson, J.M., 1993, *A&A*, 271, 697
- D'Addario, L., et al., **ALMA memo** 445 (2003).
- Hirata, A., et al., *Electron. Lett.* **38** (2002) p. 798.
- Holdaway, 1990, in ALMA memo series, No.61
- Holdaway, 1997, in ALMA memo series, No.178
- Iguchi, S., Okumura, S. K., Okiura, M., Momose, M., & Chikada, Y. 2002, in **URSI**, Recent Scientific Development , (Maastricht: URSI), J6.P.7
- Ishibashi, T. et al., *Tech. Dig. Ultrafast Electronics and Optoelectronics* (1997) p.166.
- Ishiguro, M., et al., 2002, in **ALMA memo series**, No.435.
- Lamb, J, in ALMA memo series, No.246
- Morita, K.-I., 2001, in **ALMA memo series**, No.374.
- Nakagawa, K., and Onae,A., *Proc. of SPIE* **Vol. 4269**, (2001) p.41.
- Noguchi, T., et al. 2001, in **ALMA memo series**, No.399.
- Okumura, S. K., Chikada, Y., Momose, M., and Iguchi, S. 2001, in **ALMA memo series**, No.350
- Payne, J. M., et al., *Tec. Dig. Int. Topical Meeting on Microwave Photonicsroc* (2002) p.105.
- Pety, J., Gueth, F., and Guilloteau, S., 2001, in **ALMA memo series**, No.398.
- Sekimoto, Y., et al., 2003, in **ALMA memo series**, No.449.
- Shillue, B., ALMA Week Victoria, June 2003.
- Takano, S., et al., *Publ. Astron. Soc. Japan* **55** (2003) p.L1.
- Ueda, A., et al., *IEEE Trans. Microwave Theory and Techniques*, **51** (2003a) p.1455.
- Ueda. A., et al., *J. J. Appl. Phys.* **42** (2003b) p.L704.
- Wright, M., 2003, in ALMA memo series, No.450.
- Yamamoto, T., et al., *Electronics Lett.* **38** (2002) p.795.